CHARACTERIZATION AND SIMULATED ANALYSIS OF CARBON FIBER WITH NANOMATERIALS AND ADDITIVE MANUFACTURING

by

Oluwaseun Omole

A Thesis

Submitted to the Faculty of Purdue University

In Partial Fulfillment of the Requirements for the degree of

Master of Science in Mechanical Engineering

Department of Mechanical and Energy Engineering at IUPUI

Indianapolis, Indiana

December 2023

THE PURDUE UNIVERSITY GRADUATE SCHOOL
STATEMENT OF COMMITTEE APPROVAL

Dr. Hamid Dalir, Chair

Department of Mechanical and Energy Engineering

Dr. Mangilal Agarwal

Department of Mechanical and Energy Engineering

Dr. Andres Tovar

Department of Mechanical and Energy Engineering

Approved by:

Dr. Likun Zhu

Dedicated to GOD, my biological and Turning Point family. As well as my Professors, Lab mates, and Mrs. Shelton

ACKNOWLEDGMENTS

First, I would like to acknowledge God and his help that allowed me to conduct research and write this thesis. If you asked me in high school if I would have ever thought I would come to Indiana, get a masters in mechanical engineering and complete writing a thesis, I would have thought you were crazy. Somehow, that's what happened! There have been many early mornings and late nights but through it all, one thing has been constant and that was Jesus. So, I have to thank God for doing this, because he did it! Next to him though is my family. They always supported me and even though I moved many miles away from home, they were always a phone call away. There were many times I needed their love and support and I truly appreciate all of the nights talking to Anu, Funmi or Titi and having a blast. My parents were also foundational to my success, seeing their work ethic, working 12-16hrs a day with me and my sisters growing up helped me to continue pressing during the tough days working on an assignment or in the lab doing research. I would also love to acknowledge my spiritual family at Turning Point Family Worship Center and my leaders, Pastor and Sister Harris. I thank God that I was able to meet a beautiful group of people and have grown so, so much there. There were no shortage of tough days, but coming to TP always made it better.

Academically, I would like to thank my professor and mentor Dr. Hamid Dalir. I have known Dr. Dalir for five years now and I can say that I have been blessed working under him. He allowed me to work on projects, as a freshman that many seniors would not have had the opportunity to. I was also able to talk with him about my project, and although it was difficult sometimes, I am truly grateful for his help. I could say the same about Dr. Agarwal and his openness to allow me to work on projects I was not qualified for, under him. As the leader of INDI, I had the pleasure to experience firsthand his impact on nanotechnology through INDI and leading NSF funded summer opportunities like REU. Dr. Tovar has also been instrumental in my completion of this thesis, and when I had questions, he provided the advice I needed to get out of my ruts. Last, but definitely not least, Mrs. Shelton has had as strong of an impact on me as my professors. As the head of the Diversity Scholars Research Program (DSRP), she was the first face I got to see at IUPUI. As tough as she was on us, she truly cared for all of the scholars in the program. There were sometimes

I didn’t know what to do, and she would encourage me. I cannot fully express the immense impact that she has had on me, and my life and I can cry and say that she truly changed my life.

As for my many lab partners, there is so much I can say. First, I would like to acknowledge Pias and all of his help. Although we started at around the same time, I know for a fact that I would not have completed this project without his expertise. The same could be said of others from in Innovation Hall like, Mark, Eray, and Mariana. Your great and cheerful attitude made being in the lab that much more bearable. Others that have gone, like Reza, Nojan, and Asel were also instrumental in my development, and I appreciate their patience with me.

TABLE OF CONTENTS

LIST OF TABLES

LIST OF FIGURES

LIST OF ABBREVIATIONS

µm	Micrometer
nm	Nanometer
ABS	Acrylonitrile Butadiene Styrene
AC	Alternating Current
ASA	Acrylonitrile Styrene Acrylate
ASTM	American Society for Testing and Materials
AM	Additive Manufacturing
ANSYS	Analysis (of) Systems
DC	Direct Current
EHD	Electrohydrodynamic
HV	High Voltage
2D	Two-Dimensional
3D	Three-Dimensional
VC	Critical Voltage
CAD	Computer Aided Design
CF	Carbon Fiber
CCF	Chopped Carbon Fiber
CFRP	Carbon Fiber-Reinforced Polymer
CFRCLS	Continuous Fiber Reinforced Composite Lightweight Structures
CNT	Carbon Nanotubes
DDM	Direct Digital Manufacturing
DMF	Dimethylformamide
DIC	Digital Image Correlation

E	Elastic Modulus
EMI	Electromagnetic Interference Shielding
ENF	Electrospun Epoxy Nanofibers
FAA	Federal Aviation Administration
FDM	Fused Deposition Modeling
FEA	Finite Element Analysis
GFRP	Glass Fiber- Reinforced Polymer
GHz	Giga Hertz
GPa	Giga-Pascal
GRP	Glass Reinforced Polymer
Hz	Hertz
ILSS	Interlaminar Shear Strength
kN	Kilonewton
kV	Kilovolt
MCF	Milled Carbon Fiber
MHz	Mega Hertz
MPa	Megapascals
ml	Milliliters
mm	Millimeters
L	Length
PA	Polyamide
PAN	Polyacrylonitrile
PC	Polycarbonate
PLA	Polylactic Acid
PVA	Polyvinyl alcohol

RPM	Revolutions per minute
ROM	Rule of Mixtures
RAE	Royal Aircraft Establishment
s	Seconds
SD	Standard Deviation
SEM	Scanning Electron Microscope
SLS	Selective Laser Sintering
STL	Standard tessellation language
TGA	Thermogravimetric Analysis
W	Width

ABSTRACT

Due to the vast increase and versatility of Additive Manufacturing and 3D-printing, in this study, the mechanical behavior of implementing both continuous and short carbon fiber within Nylon and investigated for its effectiveness within additively manufactured prints. Here, 0.1wt% of pure nylon was combined with carbon nanotubes through both dry and heat mixing to determine the best method and used to create printable filaments. Compression, tensile and short beam shear (SBS) samples were created and tested to determine maximum deformation and were simulated using ANSYS and its ACP Pre tool. SEM imaging was used to analyze CNT integration within the nylon filament, as well as the fractography of tested samples. Experimental testing shows that compressive strength increased by 28%, and the average SBS samples increased by 8% with minimal impacts on the tensile strength. The simulated results for Nylon/CF tensile samples were compared to experimental results and showed that lower amounts of carbon fiber samples tend to have lower errors.

1. INTRODUCTION

From building houses brick by brick to multi-billion dollar stadiums, the ability to build layer by layer has been integrated into human nature. Additive manufacturing allows machines, also known as printers, to do the same, creating diverse structures quickly and efficiently. These printers are relatively new and many researchers and companies have been pushing the limits of these tools this technology. The mechanical properties of many of these prints are much less than similar parts made with different manufacturing techniques, so researchers have turned to nanotechnology. Materials within the nano to micrometer range have much greater stiffness and strength than traditional materials. The incorporation of these nanomaterials as reinforcements has been shown to create a more substantial material.

Currently, certain companies manufacture filaments that incorporate short fibers with virgin materials to increase their strength. However, this automated process is very complex, time-consuming, and expensive. Because of this, few commercial printers can create and print both continuous and short fiber-reinforced prints. Researchers tried to replicate the industry and have been able to develop similar short-fiber filaments. However, their heavily modified printers have low scalability, limiting the feasibility of their use. As a result, a very challenging issue for 3D-Printing is using continuous and short fibers for additive manufacturing. The relative infeasibility of creating cost-effective filaments that can further increase structural strength hinders progress in this area.

However, previous research has shown that dry mixing is able to adequately coat filaments with short fibers and can be printed along with either the more muscular continuous fibers or individually for greater printing flexibility. But this incorporation is novel and still needs to be optimized. Our previous research has shown that carbon nanotubes can be incorporated within continuous carbon fiber and epoxy resin [1-3]. Thus, this thesis studies the reproducibility of uniform short fiber-filled Nylon that will be reinforced with continuous carbon fiber and tested for its mechanical properties. The simulated analysis will also be used to compare experimental findings.

1.1 Literature Review

1.1.1 The History of Carbon Fiber and its Applications

To understand the importance of carbon fiber, it is imperative to understand the history behind its creation. Sir Joseph Wilson Swan was coined as the father of the carbon fiber industry after he invented new incandescent light bulbs with carbonized paper as the newly used filament [4]. The American chemical inventor and businessman Thomas A. Edison commercialized carbon filaments in his light bulbs. Using carbon filaments allowed his bulbs to last for over 1200 h in his patent Electric-Lamp (U.S.P. Office, 1880). Minor discoveries in the use of carbon fiber were uncovered in the early 1900s. Still, the next major milestone for carbon fiber was Roger Bacon's discovery of graphite whiskers in the later 1950s. These thin cylindrical-like layers of graphene laid the foundation of what we know today as carbon fibers, as Bacon discovered that when graphite was heated to arc temperatures, they formed incredibly strong and flexible filaments [5].

In later years, Bacon also uncovered further discoveries with the microstructure of graphite [6], further aiding our current knowledge of carbon fibers. One of such discoveries Bacon and Wesley Schalamon patented was the use of creating carbon fiber by heating rayon and implementing a new method of stretching these fibers at temperatures as high as 2800°C, which resulted in more excellent Young's modulus [7].

On the other side of the globe, researchers were uncovering the intricacies of carbon in tandem with Bacon. Polyacrylonitrile (PAN), acquired by Dr. Akio Shindo was researched in 1959 and it was discovered that it produced the most significant increase in mechanical properties. Shindo delved deeper in order to compare oxidized PAN fibers to non-oxidized PAN fibers which helped uncover that the oxidized fibers were better when simultaneously carbonizing a vast array of carbon fiber batches [8]. After this discovery, William Watt and William Johnson, under the Royal Aircraft Establishment (RAE), spearheaded the commercial use of high strength carbon fibers in 1963. It was discovered that heating the PAN fibers to 2500° C nearly tripled ,its stiffness and restricting the PAN fibers during oxidation allowed widespread production lines to be implemented by 1966 [9].

These discoveries pushed PAN-based fibers into being the primary method of forming carbon fibers, even currently forming 90% of all commercially used carbon fibers. Rayon was first used to create high-strength carbon fibers in the 1960s. However, these produced low tensile strength and Young's modulus relative to the other materials. Rayon is a cellulose-based carbon fiber, that is, known for having defects such as extensive void contents and interfilament bonding [10]. However, a better method of creating usable carbon fiber was through another material called Pitch, which is derived from petroleum asphalt, coal tar, or polyvinyl chloride. Pitch-based carbon fibers can be formed into either isotropic-pitch based or mesophase-pitch-based carbon fibers [11]. In spite of this, only mesophase pitches are commercially used to create carbon fiber. Pitch is typically used to create high-modulus fibers that many critical military operations need, while PAN allows for high-strength fibers. Currently, about 90% of the carbon fiber used is PAN-based.

These three materials have led to a critical shift in the use of carbon fiber as a material in popularity, similar to aluminum, primarily due to the material's lightweight and strength properties. Despite its humble beginnings, using carbon fibers in structural applications has transformed this material into a multi-billion dollar industry [12-16]. Due to its increase in popularity, the PAN-based CF industry has been estimated to grow by 10% per year [8]. Increasing its global market from $3.7 billion in 2020 to $8.9 billion in 2031 [17]. This percentage increases within the construction industry, where estimates of its global usage increase by 12% [18]. However, due to the recent COVID-19 pandemic, the production of most composite businesses was halted with decreased production, increased costs, and material and labor shortages.

The Applications of Carbon Fiber

Let's discuss present-day carbon fiber uses and how their versatility is displayed around the world. In recent years, (carbon) fiber-reinforced plastics usage within concrete has been investigated globally ([19-22]). In Asia, tests have been conducted on the effects of carbon fiber on their structures to replace steel ([23, 24]). The automotive industry also recognizes the application of composites, like carbon fiber, for introducing lightweight structures [16, 25-27]. As the price of CFRPs decreases yearly, composite usage is becoming more and more cost-effective. The main

drawback of CFRPs is their ability to meet the needs of high-volume manufacturability or low downtime production.

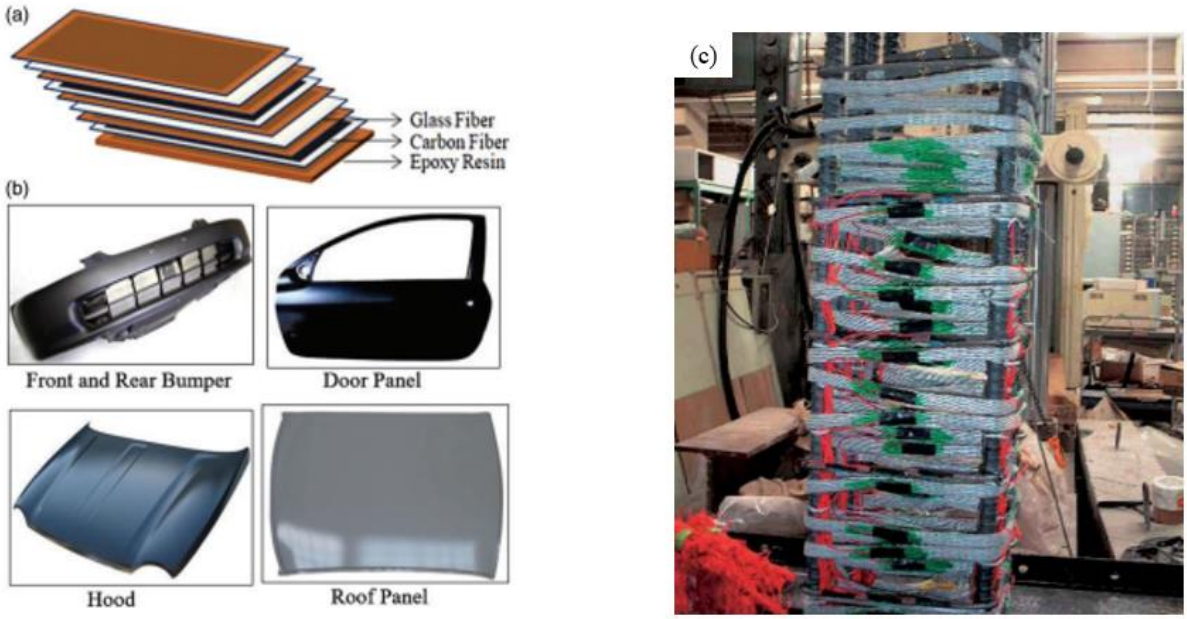

Figure 1.1: Schematic of (a) CF/GF/Epoxy composite hybridization, (b) Automotive components that are able to be converted from traditional materials (c) The use of continuous fiber in tie reinforcement [19].

Despite this, CFRPs are desired for their superior mechanical and structural properties relative to traditional materials [28]. In fact, when three Korean manufacturing companies joined together to create a CF battery pack module carrier, they experienced a 26% weight reduction, better recyclability, and cost reductions relative to a standard steel carrier [29]. Carbon fiber composites have also found their way into the sporting industry once their price decreased to 100 Euro/kg [30]. Super lightweight bicycle frames, tennis rackets, and kayaks have been formed with carbon fiber prepreg. Even sensors and detection systems have been researched, aiming to create sensors that detect deformations within composite structures.

The aviation and space industry are also looking[31] at the key advantages that CFRPs have, especially Boeing and Airbus. 50 wt% of their newer airplanes, such as the Boeing 787 and Airbus 350, are composed of composites, which they have been using since the start of the 1980s [32, 33]). Aerospace manufacturers claimed that the use of these composite materials would help lower

operating costs by 20% and lower greenhouse gas emissions by 25% [34]. Even other classes of airplanes, specifically privatized aircraft, have responded to this dramatic change from aluminum to composites. Through this, planes can take advantage of carbon fiber's high heat capacity and low density to create brake disks that are 40% lighter and last twice as long as traditional steel brakes [35].

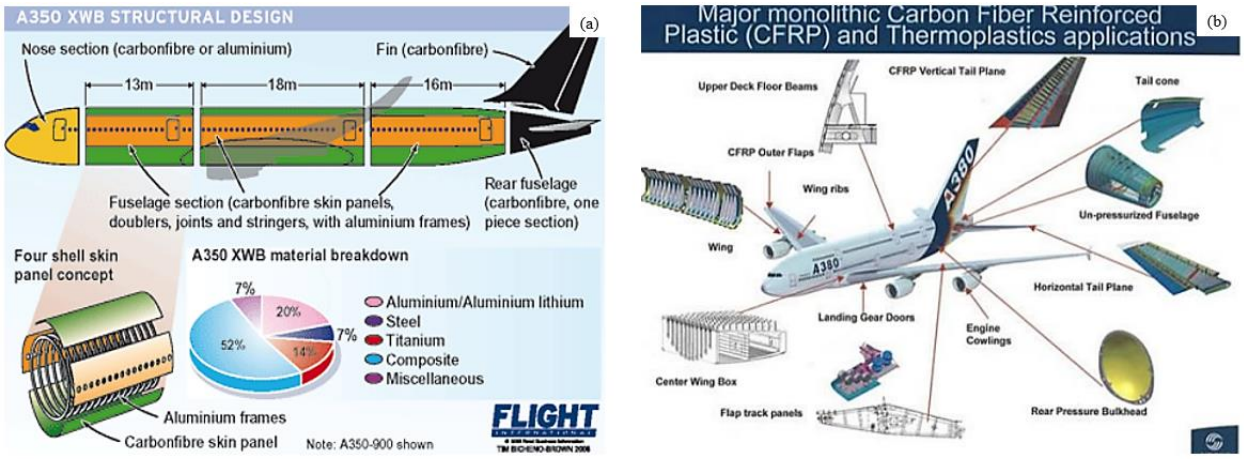

Figure 1.2: Visual representations of (a) the Airbus A350 XWB material distribution and (b) the Airbus A380 composite usage [27]

The defense and space industry has invested significant stakes in CFRPs and their high strength-to-weight ratio. The British Aerospace Defense has spent the last 50 years developing and implementing carbon fiber composites within their war-fighting planes, all to bluster their defenses and air superiority [36]. The Moscow-based company AeroComposit is one that is focused on researching and applying more robust components like carbon fiber within Russian aircraft for next-generation, single-aisle aircraft [29]. Due to stipulations put forth by the FAA, increasing thickness or radically changing aircraft internal features in favor of increased strength and mechanical properties incurs costly impacts on composites while maintaining a factor of safety. These issues are important to the aerospace and defense industry [37].

1.1.2 History of Nylon

Polyamide 6 (polycaprolactam or PA6) was researched by J. Von Brown at Gottingen University during the period of 1905-1910 [38]. While working for IG Farben in the late 1930s, Paul Schlack

filed patents for the conversion of caprolactam to Polyamide 6 through catalytic polymerization. Here PA6 was manufactured by IG Farben under the trade name, of Perlon with full-scale production completed in 1941.

Dr. Wallace H. Carothers and Dupont spearheaded commercial Polyamide after Dupont hired Carothers in 1928 and grew to become the first engineered plastic, garnering, much success during the 1950s [39]. After Carothers began at Dupont he was tasked to study long-chain polymers and after much success, he was tasked to develop Nylon 6,6 and its first sample was created in 1931. Dupont began commercial production of Nylon 6,6 in 1935 and Carothers filed a patent for stockings made of the same nylon in 1937 and an upscalable process to produce the polymer allowed Dupont to begin mass production by September 1938, and it was officially named "nylon." Nylon proved to be an instant success, selling nationwide in 1940 and was able to be appropriately fitted compared to previous synthetic fibers that became baggy when customers wore them. Nylon was also used as parachutes and body armor for the US when WWII broke out. By 1948, Nylon had expanded to be reproducible in 6 products and 12 varying colors.

Nylon 6 and its Applications

Since its creation, Nylon 6 has attracted much attention from manufacturers and researchers alike. The main use of Nylon 6 can be found in apparel, carpets, textiles and industrial applications for high-strength strands. Currently, there has been much research on the production of Polyamide with various reinforcements. Because nylon has been commercially available for nearly a century now, much of its physical, molecular, and electro-thermal properties have been well established. Hybrids of polymer/clay nanocomposites have been shown to produce significantly improved mechanical properties relative to pristine polyamide [40]. In one aspect, it could be said that much of nylon's attention as a nanocomposite is due to Toyota's use in the 1990s [41]. Here, Nylon 6/ clay nanocomposites were used to make timing belt housings during the automotive process, showing the versatility nylon has with nanomaterials.

Recent studies confirm this sentiment, as alumina (Al_2O_3) was inputted into PA6 filaments to determine the single, double, and triple particle size of alumina and it was found to create samples with greater Youngs modulus and tensile strength [42]. When conducting selective laser sintering

(SLS), powders of PA can be produced and tested to create parts with excellent mechanical properties. Various weight percentages of carbon black were inserted within PA12 and showed increased mechanical, electrical, and thermal properties reaching a maximum at 3 wt% [43]. Nanosilica was also inputted into PA12 using the dissolution-precipitation process and showed an increase in impact strength, tensile, strength and modulus [44]. Nylon has even been mixed with iron through a melt mixer, having particle sizes ranging from 50-80µm, extruded into filaments and finally tested [45]. More of these combinations will be discussed in section 1.2 of this paper.

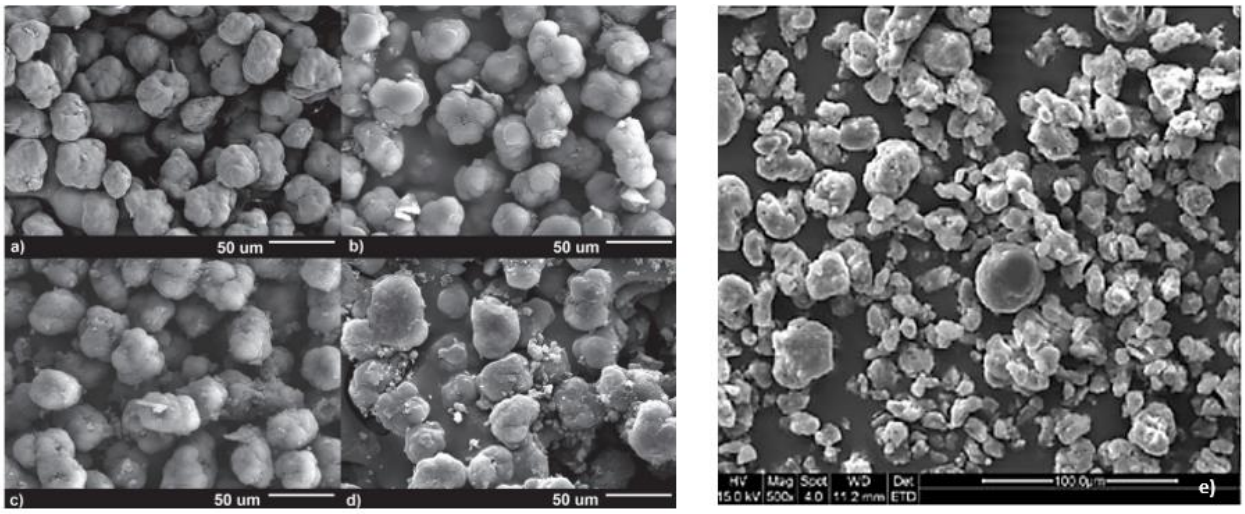

Figure 1.3: SEM Images of CB/PA12 at a) 0 wt.% b) 1.5 wt.% c) 3.0 wt.% and d) 5.0 wt.% [38]. e) SEM images and distribution of D-Nanosilica/PA12 SLS particles [39]

1.1.3 History of FDM and 3D Printers

Fused deposition modeling, also commonly known as 3D-Printing, has taken a vital role in the manufacturing industry. Many believe that additive manufacturing was first realized by Charles Hull in 1983 when he created the first ever 3D printed part and coined the term stereolithography. Hull patented his invention in August 1984, and it was awarded in March 1986 [46]. Hull then co-founded 3D Systems in 1986, gaining contracts and customers by ensuring he would not invoke his patent rights.

Because of this, through the last half-century, fused deposition modeling has developed manufacturing techniques that are widely used within many industries and diverse from other styles of manufacturing – namely subtractive manufacturing and injection molding. Additive

manufacturing is incorporated into all processes that generate a final product by erecting feedstock onto a substrate [47]. Due to its increased versatility and technical advantages, FDM can create complex structures that were previously impossible or impractical with other techniques, all with customizable parameters that the user defines [48]. These parameters can change the feedstock height, extrusion rate, nozzle temperature, and infill amount. Because of this, the demand for FDM materials and products has significantly increased, with estimates from $1.74 billion in 2011 to over $18 billion in 2022. Forty years after the first commercial printers were available, a market growth rate of over 22% has been consistently shown with more than 200 companies competing for their share [49].

The majority of materials currently used in additive manufacturing can be divided into two different polymers: thermoplastics and thermosets. Thermosetting polymers begin as soft and viscous, then irreversibly hardened or cured. This curing process can be attained naturally or through the use of a catalyzing agent, pressure, temperature or another case. Thermoplastics are the opposite of thermosets and are able to be melted, molded, and remelted again. The procedure for incorporating thermosetting polymers in additive manufacturing has only recently begun piquing the interest of researchers, due to its irreversible nature. For these reasons, this paper will primarily focus on thermoplastics.

FDM is a part of additive manufacturing (AM), the manufacturing technique that builds materials on top of itself layer by layer. AM can be divided into many subtypes: Fused Deposition Modeling (FDM), Selective Laser Sintering, Laminated Object Manufacturing, and Stereolithography. Most professionals and hobbyists turn to FDM, also known as 3D-Printing, and by using this method, components are formed by layer-by-layer addition of a melted polymeric matrix. This method offers the potential of significant cost savings [50], quick material change [51], quick production speed [52], as well as potentially large-scale prints [53] relative to other AM subtypes. Before printing begins, a virtual drawing of the print is created, and this STL file is sliced into horizontal layers to enable further customization of the print's parameters [54]. Some of these parameters include layer height, print speed, infill percentage, wall thickness and much more. Because of this versatility, FDM has been used for aerospace, civil engineering, food production, sports and others [55].

When beginning the printing process, filaments of meltable thermoplastics are inserted into an extruder, where it is heated past its glass transition temperature. At this point, the melted plastic is extruded through the extrusion nozzle, with the nozzle head moving through the path that was dictated by the slicing software accordingly and its parameters. The nozzle deposits the first layer of material on the print bed, which typically can be heated for better print quality, and after it completes this first path the bed moves down for another layer. This process continues, additively increasing the size of the print by the print's layer thickness until the print is complete. This process can be seen below in Figure 1.4b.

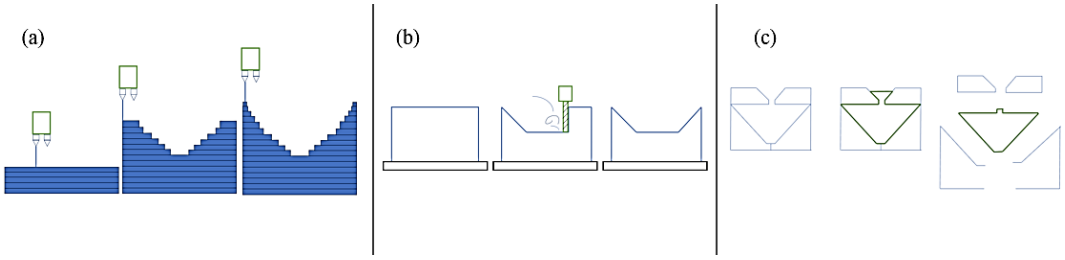

Figure 1.4: Schematic of the following manufacturing processes: a). Fused Deposition Modeling, and b). Subtractive Manufacturing, c). Injection Molding

1.1.4 Single and Multi-Nozzle 3D Printers

One niche area of FDM is additively manufacturing two more materials. Over the past decade, more and more printers have been introduced with the capability of printing with either two materials and colors or one structural material with dissolvable support materials to create complex parts. Composites of two or more materials are being explored for their structural properties, garnering much interest from companies and academic researchers. However, incorporating different FDM materials is not as simple as it seems. Quality issues such as, large processing times [56], voids, surface finish, and poor material adhesion tends to plague these types of printers and its creations. Researchers have spent much time and effort minimizing these drawbacks and one such way is with the use of nanomaterials.

1.2 Current Technologies Incorporating CF

1.2.1 FDM of Continuous Fibers

There are only a few ways a researcher or company can print with continuous fibers, and one of the main ways to do so is by creating a personal printer with that capability. In this section, I will review numerous studies combining unidirectional fibers with thermoplastics to create mechanically more robust prints. These continuous fibers are able to reinforce the thermoplastics in the x or y-direction or a combination of the two, allowing for prints that can be used in greater, more structural applications.

Researched Continuous Fiber Incorporation

In a study by X. Tain, continuous carbon fiber was used to reinforce polylactic acid (PLA) as the reinforcement and matrix, respectively [57]. PLA and continuous carbon fiber combinations were created using an individually developed 3D printer and various parameters to test their effects on a print's mechanical properties. These parameters included: liquefier temperature, layer thickness, feed rate, hatch spacing and printing speed. Increasing the melting flow index (MFI) increased carbon fiber impregnation within PLA, therefore increasing mechanical strength. Flexural strength was also shown to increase with a higher feed rate but decrease with higher layer thickness, printing speed, and hatching speed. It was shown that with optimized parameters, carbon fiber reinforced PLA can show an increase of 27% in mechanical strength, specifically achieved on a personal printer. In a follow-up study by Tain, the effects of recyclable PLA and its recovery rate to determine the mechanical, environmental, and aging effects it has compared to pristine PLA [58]. PLA and continuous carbon fiber were extruded in the same nozzle and used to create test specimens for comparison, and no significant increases in tensile strength were found when using pristine PLA against its recycled counterpart. However, remanufactured PLA showed a rise of 25% in flexural strength and an 8% decrease in flexural modulus, with the Charpy impact strength increasing as well.

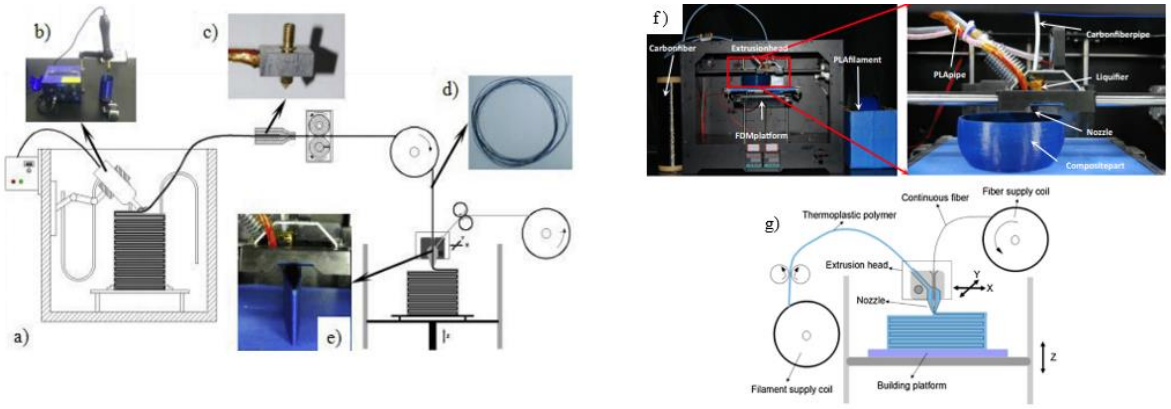

Figure 1.5: a) Complete schematic of the remanufacturing process: b) Hot air gun, c) remolding nozzle, d) obtained filament, and e) final print [53]. f) Print and critical components of the printing mechanism, g) representation of the printing process.

Matsuzaki also looked into the possibility of an independent printer that can print diverse thermoplastics and reinforcement materials [59]. Here, a printer with controllable fiber direction and volume fraction was created with straight tows of carbon fiber and twisted yarns of jute fibers were used to reinforce PLA. Both were extruded at temperatures of 210℃ and at different speeds to prevent fiber stacking. Tensile test specimens were created and tested in accordance to JIS K 7162 with carbon and jute reinforced specimens exhibiting a 599% and 157% increase in modulus as well as a 435% and 134% in tensile strength. It was also shown that fiber pullout was a problem for the researchers and inadequate resin and reinforcement adhesion prevented higher mechanical properties.

Hou looked at reinforcing PLA with continuous Kevlar to create complex structures or continuous fiber reinforced composite lightweight structures (CFRCLSs) through the use of an additive 3D printer and a motion arm with six degrees of freedom as a motion mechanism [60]. A complex spline corrugated core was created to evaluate bond failure between the sandwich structure. Experimental testing showed that the compressive strength and modulus decreased when cell length and layer thickness increased, with a maximum compressive strength of 17.17 MPa. Sugiyama followed a process similar to Hou with the aim of creating complex carbon fiber sandwich structures [61]. An independently made printer that can print composite sandwich structures without support material, printed carbon fiber continuously without a cutting mechanism

using differing shapes of the sandwich structures and unit cells. These shapes include honeycombed, rectangular, circular, and triangular filled structures. Afterwards, these structures were subject to three-point bending and tensile test and it was determined that honeycomb filled structures were the weakest with the remaining three shapes being relative in loading capability. The theoretical computations of the tensile strength and elastic modulus were also shown to be 62% and 89% relative to the experimental values. Chen also provides a simulated and experimental approach to determine the shear behavior of a carbon and Polyphenylene Sulfide (PPS) composite created using FDM [62]. For this, bias extension test was used for predicting shear behavior at high temperature. Test specimens were created using carbon woven fabrics and PPS resin, cut into 210mmx70mm rectangles and tested at varying temperatures (295, 300, 310 and 320℃) and displacement rates (5, 10 and 15mm/min). A solid-shell element was used for the proposed thermo-visco-elastic model, through which the effects of strain rate and temperature were shown. The simulated tensile force and coefficient of friction were compared with experimental values for all nine parameters.

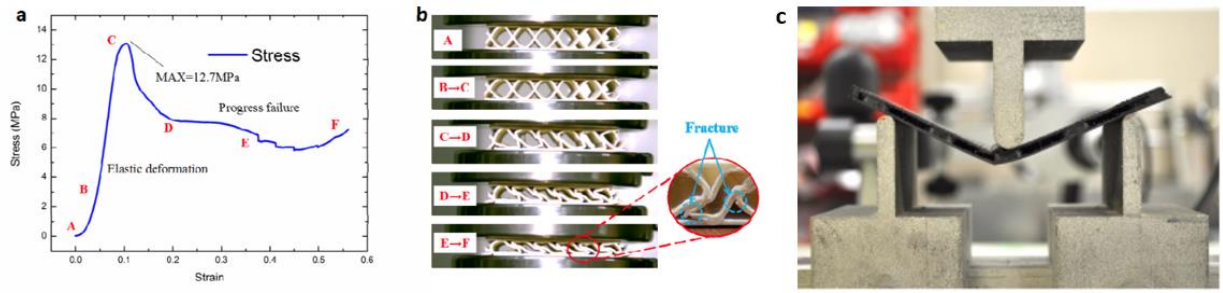

Figure 1.6: a) Stress vs. Strain load curve, b) compression sample under linear and nonlinear deformation [56]. c) Experimental image of fracture 3-point bend fracture [55]

Another popular thermoplastic that was combined with continuous fibers is Acrylonitrile Butadiene Styrene or ABS. For example, work done by Mosleh explored the creation of continuous fiber-reinforced thermoplastic composites (CFRTCs) through carbon fiber reinforcing ABS [63]. To do so, a solution impregnation method ,combined the fibers, also known as prepreg, and ABS filaments down into a singular nozzle. Three different parameters were studied: nozzle diameter, layer height and layer speed with various mechanical tests conducted. Forty one samples were produced and tested based on these parameters and all fibers printed from 0.5, 1, and 1.8mm

nozzles failed. During mechanical testing, the tensile strength of the reinforced composites was shown to increase nearly four times relative to pure ABS, and more than doubled its flexural strength. The ILSS was shown to increase by 54% and micro-voids and thin layers of ABS were shown within the matrix and the surface of the prepregs respectively. Researchers at Toyohashi University then studied the use of dieless forming during the AM process with continuous carbon fibers [64]. In this process a lower plate of ABS was printed in the form of tensile test specimens with a nozzle temperature of 190℃. After this continuous carbon fibers were placed on top of the lower plate and another upper layer of ABS was printed and heated for 15 minutes to enforce thermal bonding, creating a completed tensile test coupon. A schematic of these methods can be seen in Figure 1.7. Specimens with and without thermal bonding were made and compared with specimens without continuous fibers with thermally bonded prints reaching a tensile force of approximately 900N. Another test was conducted in which the carbon fibers were deposited with ABS within the nozzle head, and it was found that these fibers can reach a force of 1.5kN [65].

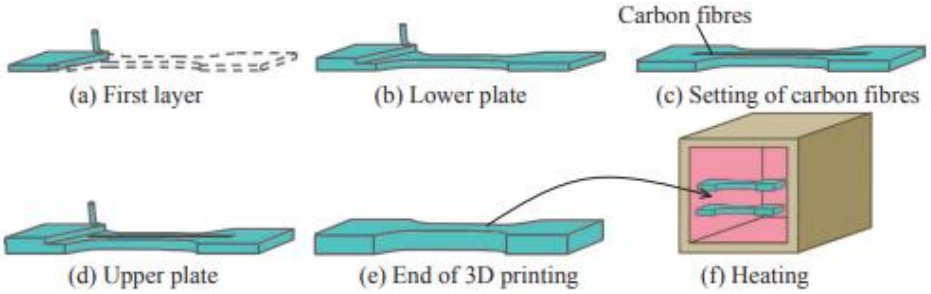

Figure 1.7: Methodology used by Mori to create continuous tensile specimens [59]

Nakagawa used a single nozzle printer to print ABS coated carbon fibers in a method very similar to Mori. In this study, molten ABS was printed from two different nozzle diameters, 0.4mm and 0.9mm, and temperatures 225℃ and 190℃ and compared. The first few layers of ABS were printed, then continuous carbon fibers were placed on top, and the second layer was printed, encasing the carbon fiber within the two sides. This methodology can be seen in Fig 1.8. Some of these tensile test specimens were thermally bonded with a heating pin before the second layer and a microwave oven afterward, but these two sample types, along with pure ABS, were tested. The finished prints were tested for their nominal stress, and the thermally bonded samples made with

the 0.4mm nozzle were stronger than samples without thermal bonding or carbon fiber. When using the three-point bend test, it was found that pieces made from the heating pin tested stronger than those bonded using the microwave.

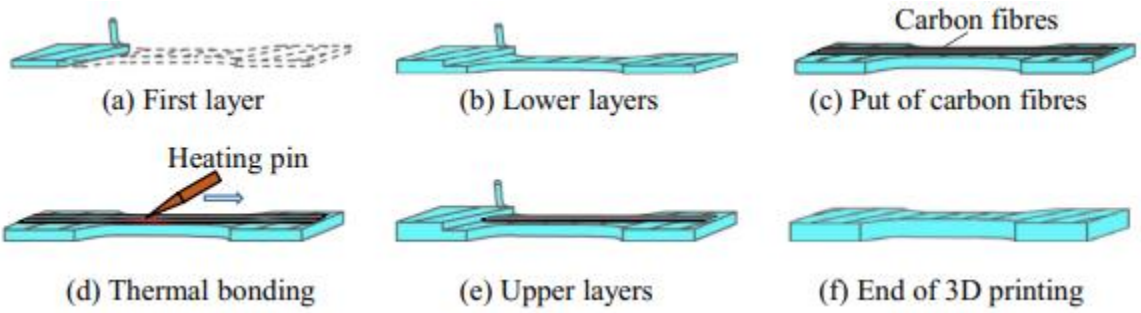

Figure 1.8: Graphic showing the methodology used by Nakagawa to create bonded ABS-CF samples [60]

Finally, Fujihara et al. used continuous carbon fiber to reinforce Polyethertherketone (PEEK) to replace thermoset composites in high-stress applications [66]. This study used the micro-braiding method to create flexible thermoplastic composites by combining three middle-end-carbon fibers with 10 PEEK fiber yarns in a diamond braiding structure. Then PEEK/Carbon plates were made by compression molding at three different holding temperatures: 380, 410, and 440℃ and three different holding times: 20, 40, and 60min. The bending strength and modulus were analyzed using finished four-point bend testing and were observed using thermalgravimetric analysis (TGM) and SEM. It was discovered that the bending strength and modulus were impacted at 440℃, and TGM implied that PEEK interface degradation occurs with higher holding time and temperature. The optimum time and temperature was found to be 380℃ at 20mins.

Continuous Fiber Incorporation with MarkForged Systems

Although few researchers and companies have allowed the printability of continuous fibers, one company has stood above others in this area – the MarkForged brand. MarkForged was founded in 2013 and has impacted the 3D-printing industry since then. Dickson produced a preliminary study on the mechanical strength of fiber reinforced nylon [67], studying the use of the initial MarkForged printers. Here, the initial Mark One composite printer was used to create test samples to determine flexural and tensile properties. Volume fraction was calculated using image analysis

software, and carbon fiber was further reinforced as the fiber that produces the most significant mechanical increases. It was also shown that increasing reinforcement layers for both isotropic and centric patterns increase maximum strength, with the former leading the steepest increases. Dickson later looked at the mechanical properties of woven continuous carbon fiber and its effects on open-hole tensile tests [68]. To create circular holes for this study, a fiber path generator was used, where the X and Y axis were diverted into a specific area to create a 5.9mm hole that could still be reinforced with the continuous fibers while still preventing the rise of matrix and fiber alteration or matrix-rich sites. Three different specimens were used to create a hole within a test specimen: tailor woven, die punching/drilled, and standard unnotched specimens, viewable in Fig 1.9a & 1.9d. The tensile test was conducted under American Society for Testing and Materials (ASTM) D5766, and DIC imaging was used for post-testing strain analysis. As expected, the maximum principal strain was significantly higher for die-notched (44mS) and tailor woven (24mS) specimens relative to samples without holes. The ultimate tensile stresses were reduced by 49% for die-punched and 93% for tailor woven specimens. SEM imaging inferred that crack arrest was shown for the tailor woven samples, while the die-punched sample did not, which may have allowed for faster crack propagation.

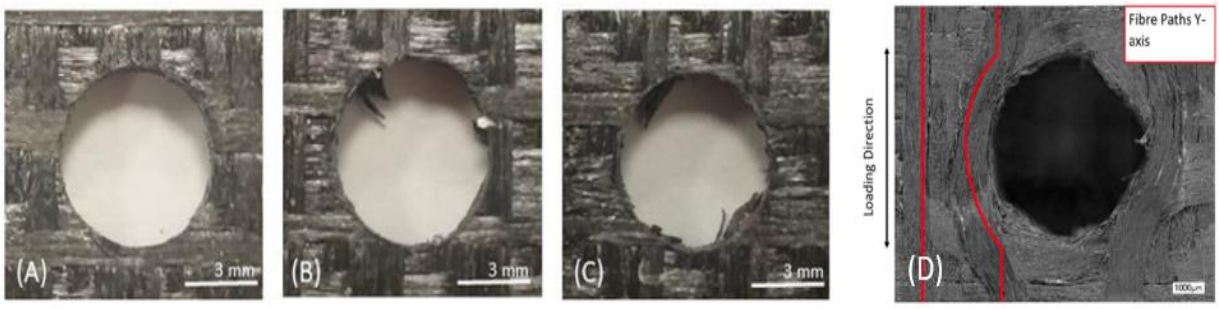

Figure 1.9: Visual of various drilling parameters at a feed rate of 53cm/min: a) 7500 RPM, b) 2800 RPM, c) 1600 RPM. d) fiber pathing and load distribution for FDM printed samples.

Spanish researchers M. A. Caminero et al. studied the influence continuous fiber reinforcements had on the impact strength of an additively manufactured print [69]. To do so, glass Kevlar and carbon fibers were used to reinforce PA 6, and they chose to study the effects of three parameters: build orientation, layer thickness, and fiber volume. The test specimens were oriented either on their back or on-edge, with layer thicknesses of either 0.1, 0.125, or 0.2mm at 100% rectangular

shape infill. After five test specimens were created for each parameter, Charpy impact tests were conducted under ASTM D6110 standards, and it was shown that glass fibers exhibited the most significant impact strength at 280.95 kJ/m^2. SEM imaging showed the poor wettability of Kevlar and carbon fibers with the nylon and the fact that Charpy samples that were printed on-edge were presumed to be caused by air void and higher porosity. Researchers in Mexico and Spain then joined forces to determine the effects of process parameters, such as print speed, print temperature, and geometric variables, with mechanical strength [70]. To do so, they used: pure Polyamide 6 (PA6), PA6 strengthened with chopped fibers (called Onyx), and PA6 reinforced with continuous carbon fiber and converted them into three different setups. Setup 1 was base PA, Setup 2 was onyx, and Setup 3 was reinforced PA6, where samples of 40, 40, and 15 test specimens were created. Tensile tests were conducted by the ASTM D638 standard, and once conducted SEM images of the test coupon and the Elastic modulus (E) were found. It was found that 70% of triangular infill onyx specimens generated an increase of 297% in strength relative to pure PA6, and the elastic modulus of a PA6 reinforced material grows to become 25times higher (from .95GPa to 23.7GPa).

Other researchers, such as Ply, also experimented with open-hole continuous carbon fiber and stress concentrations for aerospace applications [71]. In this study, continuous carbon fiber was used with nylon to make two testing geometries, rectangular and dumbbell/circular shaped, which were tested under two types of holes – a printed 5mm hole and a drilled hole. The dumbbell-shaped and rectangular prints were of different thicknesses, which dissuaded the authors from measuring stress. There were three main fracture analysis modes: fracture mechanics, point stress criteria, and progressive damage models, and digital image correlation (DIC) was used to determine damage propagation. This was used to show the strain at 18kN and 14kN for both hole shapes and the longitudinal and transverse stresses. A different open-hole test was conducted to determine the effect of reinforcement around a circular hole. The printed specimens with a 5mm hole were layered four ways. Of these ways, the various reinforcements experienced a decrease in maximum tensile stress by 75-85% and were compared with existing literature and were found to be relative. Many other researchers claim to work on continuous fibers but fail to reverify if their prints are still continuous. Ply addressed this and inferred that this caused a decrease in strength in their prints.

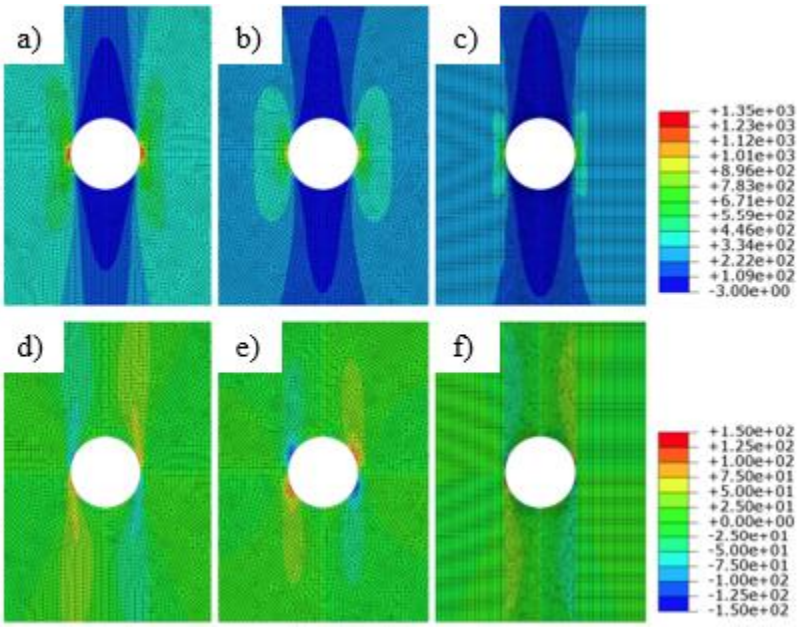

Figure 1.10: ABAQUS longitudinal stress distribution, S_{yy} of a) circular hole without reinforcement, b) with reinforcement, c) rectangular hole with reinforcement. Shear stress distribution, S_{xy} of d) circular hole without reinforcement, e) with reinforcement, f) rectangular hole with reinforcement.

Due to nylon's hygroscopic nature, its properties tend to decrease when "wet" with atmospheric water compared to when in a "dry" state. Chabaud aimed to better understand the influence sorption and absorbance has on additively manufactured polyamide as well as determining the long-term mechanical performance of PA prints [72]. PA reinforced with carbon fiber and glass fibers were noted as cCF/PA and cGF/PA and was printed at three different print layers: 0.1, 0.125, and 0.2mm. The commercially available cCF/PA and cGF/PA were shown to have beads incorporated within the filaments and could also be demonstrated in prints, as seen in Fig 1.11. Tensile tests showed that the ultimate tensile stress increased by 23 and 19 times for cCF/PA and cGF/PA, and the specific modulus increased by 137 and 67 times. The moisture uptake was tested using the Park Model, and the consequences of hygroscopic swelling were uncovered. Klift also developed ways to determine the tensile strength of continuous fibers using direct digital manufacturing (DDM), and it was tested with dry and water-absorbed polyamide. Ten 45x45x3mm samples were created for three different specimens: pure nylon, two layers of CF and six layers of CF. Pure nylon showed a tensile strength and modulus of 85MPa and 2.8GPa when

dry compared to 50MPa and 1.3GPa when wet with moisture. Samples with six layers of CF reached an average tensile strength of 464.4MPa and modulus of 35.7GPa.

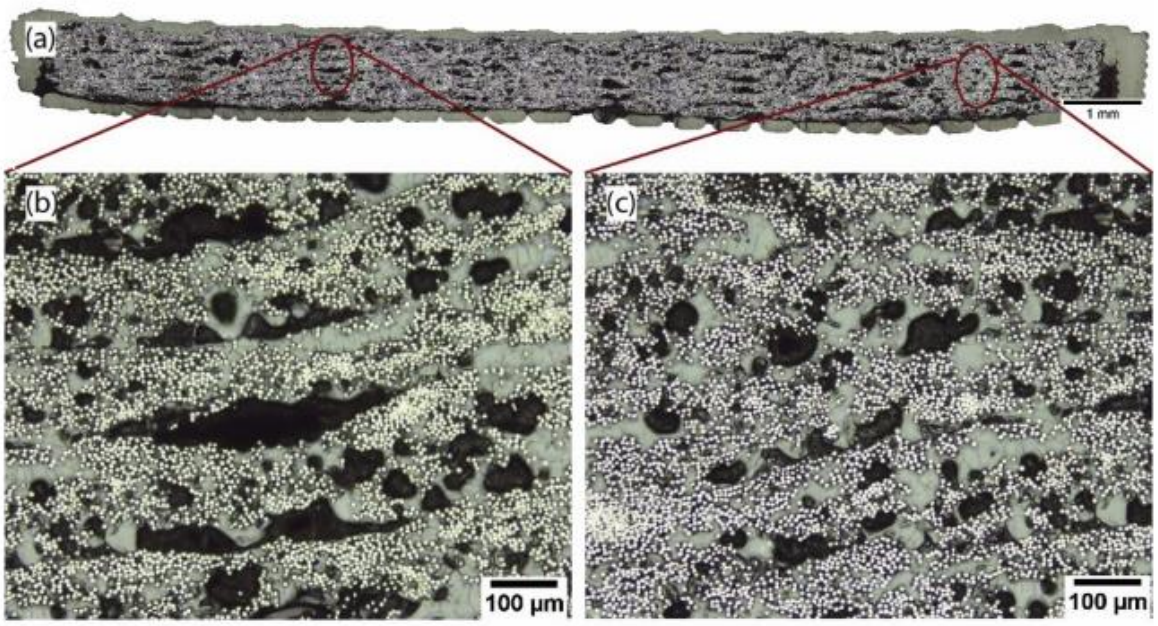

Figure 1.11: a) Panoramic view of a cCF/PA sample compiled with beads and close-up images that show intra-bead porosity [67].

Goh also looked at the mechanical properties and strength of carbon and glass fiber reinforced Nylon, with a particular emphasis on the density, porosity, and indentation properties [73]. The porosity was found in accordance to ASTM D3171- 15, using a μCT-scan showed voids larger than 16.4μm gave a void content of 2.7%, much smaller than the density calculated at 10%. The tensile and flexural test specimens were created according to ASTM D3039 and D790 respectively. It was shown that glass reinforced fibers had slightly lower tensile properties and much lower flexural properties. However, glass fiber prints were shown to be more challenging, having better impact resistance and strain than carbon fiber prints. When determining the effects of infill type, researchers at Tennessee Technological University further discussed the failure modes of continuously reinforced nylon [74]. Nylon was reinforced with unidirectional Kevlar, carbon, and glass fiber and analyzed using creep, fatigue, and tensile tests. The test specimens were created by ASTM standards, with 50% infill, dried for two hours before printing and testing, and tested both 25℃ & 100℃. Carbon fiber with an isotropic and centric infill was stronger in tensile strength

than all other types of infill. Generally, it displayed the best fatigue life relative to fiberglass and Kevlar. SEM imaging showed that large void areas served as the basis of crack growth due to low interlayer adhesion. Justo then uses the MarkForged printer to create test coupons for the mechanical properties and comparing the results of various volume fractions [75]. The tensile tests of carbon and glass fiber specimens were 250x12.5x1mm and 175x25x2mm, at 40% and 50% volume fractions respectively. Compression specimens and In-plane shear stress were printed, and for all mechanical properties, carbon fiber enhanced prints showed more excellent properties than glass fiber prints. However, when these prints are compared with traditionally created prepreg carbon and glass fiber, the difference in strength can be up to two – six times.

1.3 Computational Analysis of FDM Continuous Fibers

There are many ways a researcher, company, or hobbist can use a 3D printer, but what if material prices are too high or there are delays? How can one predict the behavior of a material that they do not have? This is where computational analysis comes in. This type of analysis occurs when computers and their systems are used to evaluate input data for specific parameters. Through this, multi-scale modeling systems can model and simulate physical things virtually. Finite Element Analysis (FEA) has caught the attention of many researchers and companies, as prints' mechanical, electrical, and thermal properties can be estimated before printing even begins, saving time, effort, and money.

For example, one FEA software is MSC.NASTRAN and Werken studied the microstructure and estimated the mechanical properties of 3D-printed continuous fibers [76]. Five samples of reinforced prints were used and tested by ASTM D7028, where the strength and modulus of these parts were within 5% of the manufacturer’s results. For Type II tensile tests, the simulated values of normal stress was only 1.3% larger than the experimental results. However, when using the rule of mixtures (ROM) as a base, all experimental specimens failed with gauge stresses 30-50% lower than ROM. Using FEA, it was discovered that models with larger concentric reinforcement filament rings had higher shear stress than those with lower rings at the failure location. These locations typically occurred during the necking portion of the sample and can be shown in Fig 1.12. Overall, the mechanical FDM process and the presence of voids causes failure quicker than

simulated results. More results like Werken's can be found with other software like ANSYS and ABAQUS will be further explored below.

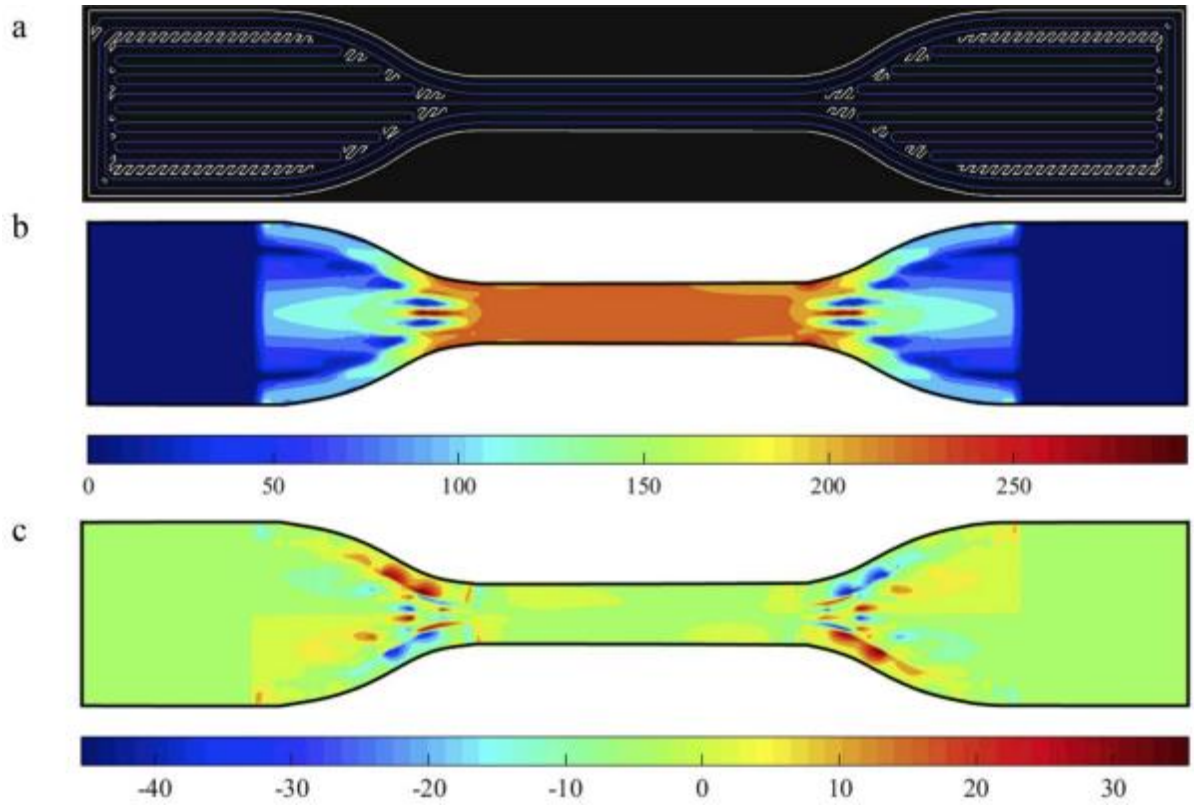

Figure 1.12: Tensile test type II a) Slicer geometry and infill settings b) Normal stress at failure c) Shear stress at failure [71].

1.3.1 Computational Analysis through ANSYS

In Norway, Ghebretinsae looked at the correlation between numerical and experimental values of the Markforged printer and its continuous prints using ANSYS [77]. Here, continuous carbon fiber and nylon were tested according to ASTM D3039 and D-7264M, and the fiber volume fraction was calculated using the rule of mixtures (ROM). When using ANSYS, many assumptions were made, such as linear elastic behavior, assumed material properties, isotropic fibers, and perfect adhesion between the fiber and nylon matrix. Despite this, the average maximum tensile and flexural strength was found to be 560 MPa and 271MPa, respectfully. When comparing the elastic modulus, experimental results showed 16GPa compared to the much higher 25GPa that was virtually calculated, showing the effects of these assumptions. Žmindák aimed to accomplish the same with a lower percent error and used ANSYS as well to conduct FEA of nylon and continuous

carbon fiber test coupons [78]. They used the software ANSYS Composite Pre/Post, also known as ACP, to simulate their tensile test. The appropriate boundary conditions and degrees of freedom were replicated to model an experimental tensile test, and three loads of 1500N, 3600N, and 9600N were applied for specimens one, two, and three, respectfully. Deformation error between the first two samples were less than 1% but increased to nearly 34% in sample 3 due to its significant increase in strength.

In the Philippines, researchers aimed at a more practical approach when using FEA. Galvez constructed a tidal turbine blade using polylactic acid, Nylon and FEA to determine if the blade edge can withstand the static and dynamic loads it would face [79]. To conduct these experiments, tensile specimens were created using ASTM D638 standards,. The tensile strength was 577MPa, and the load-deflection curves for various infill patterns were simulated and compared, as seen in Fig 1.13. Three blades were manufactured: a solid, shell-spur, and shell-infill blade. When simulating manufacturing the turbine blade, the edges were constrained to deflect less than 160mm when imposed with a 2 m/s load and 6 rad/s centrifugal force. PLA failed this test, so Markforged Onyx and carbon fiber was used as a replacement and decreased its deflection. The optimized values for each of the three blades simulated were found at 7.5mm shell thickness, for both the shell-spur and shell-infill blade. The solid blade had the lowest deformation at 9.3mm and the other two blades both experienced 9.72mm of deformation, proving that the blades would not break.

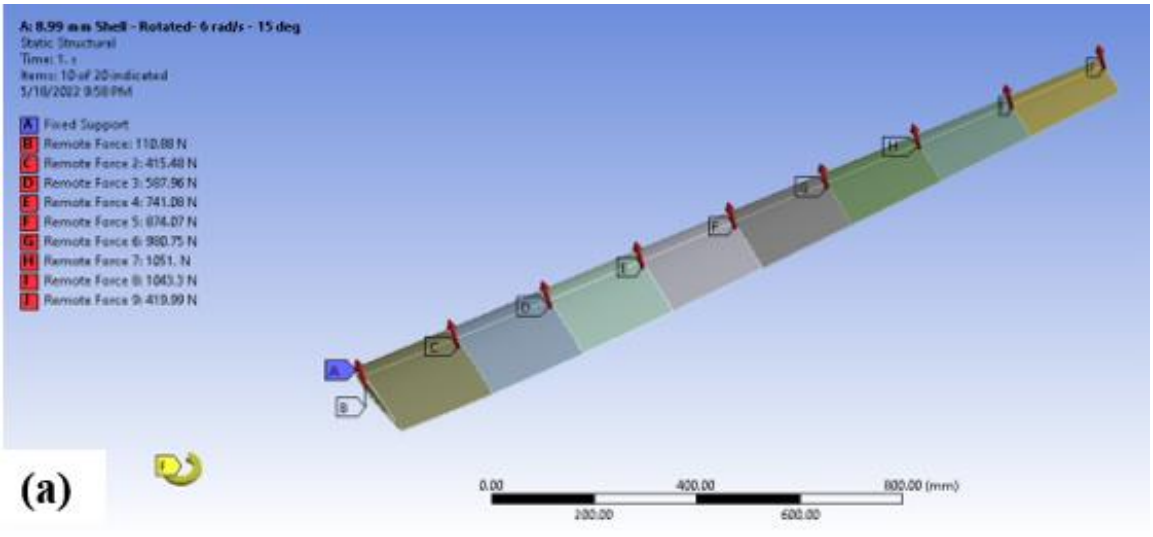

Figure 1.13: ANSYS setup and simulated loads for the wing [74]

The practical use of continuous fibers also led researchers at Romania look at the feasibility of a robotic arm created from nylon and continuous fiber glass [80]. Two FDM designs were created to simulate a robotic arm with two grippers that was CNC milled. The first design used an I-shaped cross section and the second design used a typology optimized design, with both designs reducing the arm's initial volume by 27% and 20% as well as its weight by 70%. The designs were printed, weighed and an assumed clamping force of 96N was evaluated virtually using ANSYS. It was determined that a factor of safety of 3.3 and 3.6 was determined for design one and with a deformation of 3.3mm for both. However, experimental analysis was not conducted and is needed to verify these results.

1.3.2 Computational Analysis through ABAQUS

Firstly, Avanzini looked at the use of Embedded Elements (EE), a special program within ABAQUS, to simulate continuously reinforced nylon [81]. With EE, the host, or matrix material, and the embedded parts, the fiber reinforcement, can be meshed separately with solid or beam elements. For experimental studies, rectangular specimens were created according to ASTM 3039 and several notches were included to explore the limitations and accuracy of EE. Isometric, centric and mix fill prints were also reviewed, shown in figure 1.14, and it was found that The highest loads were experienced by the unidirectional materials. The Von Mises and maximum principle stress was simulated and mapped, and when the experimental and EE stiffnesses were compared and minor differences were found. It was also found that when using EE, a linearly elastic property was assumed and more discrepancies could be found when results deviated from linearity, so further refining of these properties can increase accuracy. Savandaiah created double shear lugs using FDM and continuous carbon fiber to test the feasibility of manufactured continuous parts using the Anisoprint A4 Composer 3D printer [82]. Here, the load carrying capacity of the printed lug was initially simulated using ABAQUS and assuming quasi-isotropic and linearly elastic properties. This was then postprocessed in MATLAB and then placed into the NanoGcode software to direct the printer according to found maximum and minimum stress values. Four lugs were printed and tested using a 100kN servohydraulic test rig and DIC calculated the surface strains. Experimental testing showed that the lugs can reach a maximum principal load 11.5kN and average linear stiffness of 4.59, 2.9% higher than simulated results.

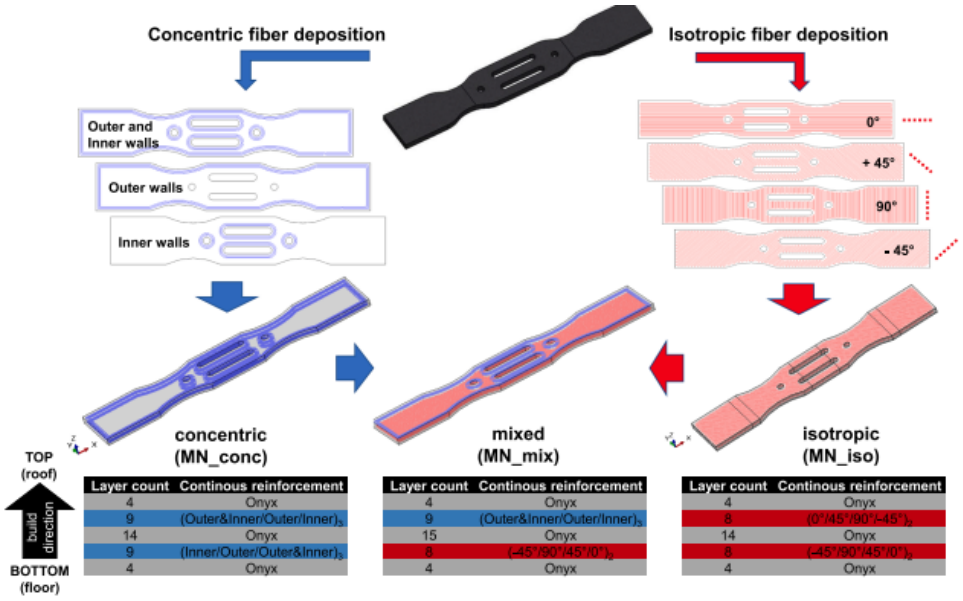

Figure 1.14: Print orientation of concentric, isometric and mixed fiber reinforcement [76]

Melenka used continuous 3D-printing to determine the effects of centric fiber rings on the mechanical properties of prints, while trying to predict said properties [83]. Here, they researched samples with 5, 4, 2 and no rings, and conducted optical microscopy with a pixel width of 1-2µm. An analytical MATLAB script was used to predict and compute the mechanical properties of these structures and the volume average stiffness method was also employed, with assumed mechanical properties taken from supplementary literature. Mechanical testing found that the elastic moduli to be 1767, 6920, 9001MPa and compared with experimentally found 4156, 7380, and 8992MPa respectively. When viewing the optical microscopy, the failure location for each sample was shown to be at the start of the Kevlar reinforcement.

Finally, Abadi et al. also looked at the use of both experimental and theoretical simulations to verify the affect build orientation has [84]. 250x25x25mm flexural coupons were created and printed axially (0º) and biaxially (0º and 90º) and it was shown that reducing the carbon fiber amount from 100% to 40% results in an axial modulus decrease of 56%, 71% and 74% for carbon fiber, Kevlar and glass fiber respectively. The software MATLAB and its ABAQUS program was used to estimate the failure modes of these prints with the help of a volume average stiffness (VAS) script. An error of 0.28%, 3.2% and 7.5% was found for the simulated elastic modulus of glass, Kevlar and carbon prints. ABAQUS was used to simulate interlaminar failure using Hashin's

damage initiation theory and the VAS method found the modulus of elasticity and Poisson's ratio with a low degree of error.

2. MATERIALS AND METHODS

2.1 FDM Methodology

In this project, four printers were used to create preliminary testing materials: the Ultimaker3, Stratasys F120& F370 and finally the Markforged Marktwo composite printer. Each of these printers have their advantages and disadvantages. This will be discussed in this section.

2.1.1 Printers

First, the Ultimaker3 is a dual extruder FDM machine, with one nozzle that exclusively prints with the water soluble Polyvinyl alcohol (PVA), named print core BB. Print core AA is used to extrude any other materials the user specifies. These print cores come in sizes 0.25, 0.40 and 0.80mm and can be switched one with another. This printer can print the following filaments: PLA, Tough PLA, ABS, Nylon, TPU, and Polycarbonate (PC) all with a filament diameter of 2.85mm. As stated before, PVA is used as support material that dissolves when submerged in water to create more intricate materials. An image of the printer and its nozzles are exemplified in Figure 2.1. Figure 2.2 then shows an image of a semi-finished print with PVA and afterward without.

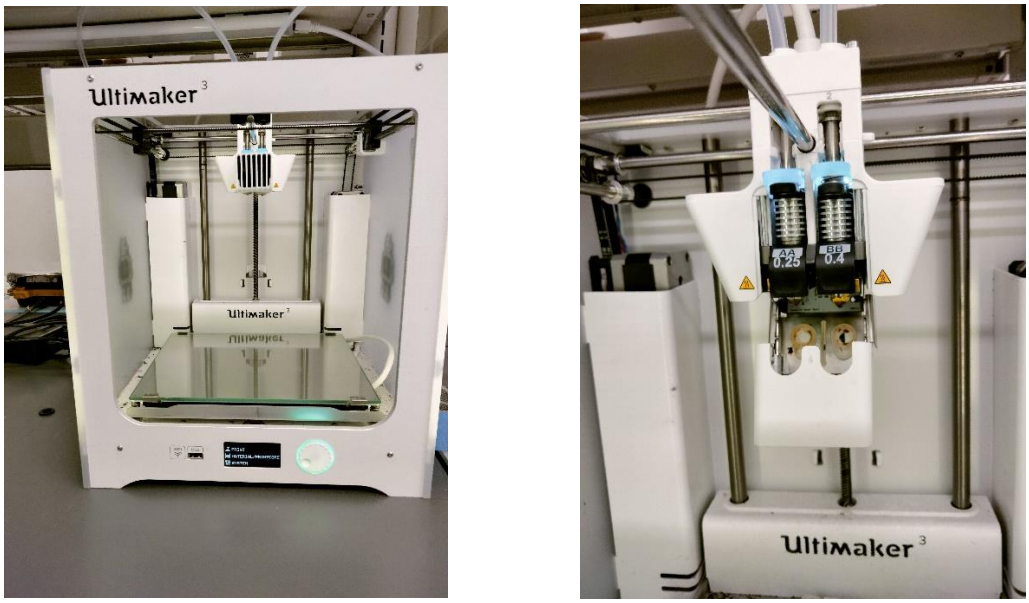

Figure 2.1: Image of the Ultimaker 3 and its two nozzles.

The Stratasys printers also prints with two nozzles, one that prints support and structural materials. The F120 is a smaller industrial printer that prints mainly ABS and Acrylonitrile Styrene Acrylate (ASA) as well as SR-30 as support materials. The F370 is a more robust printer than the F120 and can print much more filaments. Namely: PLA, ABS, TPU, ASA and more with the support nozzle printing QSR. For both SR-30 and QSR, they are both dissolved not with water, but within a dissolving apparatus. This apparatus can dissolve these support materials within the range of 50, 60, 70 and 85 ºC. Both printers print these materials with a diameter of 1.75mm.

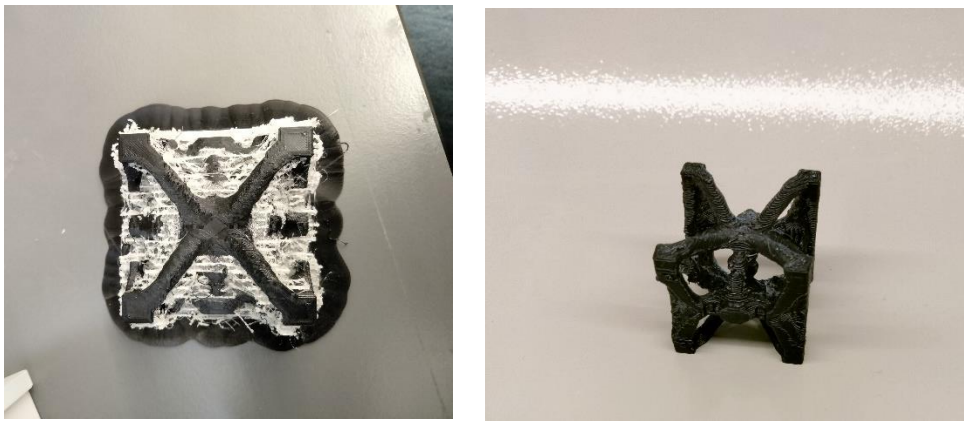

Figure 2.2: Image of a black PLA print with white PVA support and an image of the print afterward

The final printer that was used is the Markforged MarkTwo. This printer is a commercial printer that can print two structural materials. The MarkTwo uses a dual nozzle system to print both thermoplastics and continuous fibers. By adopting this system, a 0.4mm nozzle can print pure nylon, nylon reinforced with short carbon fibers (proprietorially called Onyx™) and more recently PLA and ULTEM™ 9085 filaments. The exact compositions and constituent properties of these filaments are not divulged publicly, however many mechanical and thermal properties are. Due to the dual nozzle setup, many users can purely print any of these 1.75mm diameter thermoplastics, without additional reinforcement.

If a user chooses to print using continuous fibers, they can be printed using the 0.9mm fiber nozzle in conjunction with the filament nozzle. However, the nozzles are not extruding both materials at the same time. The thermoplastic – nylon, for example, is used as the matrix that binds the

continuous fibers together, resulting in much stronger parts. Through this process, an approximate volume fraction of 30-40% is achieved. A picture of the F370 and MarkTwo 3D printers that were used are shown in Figure 2.3 below:

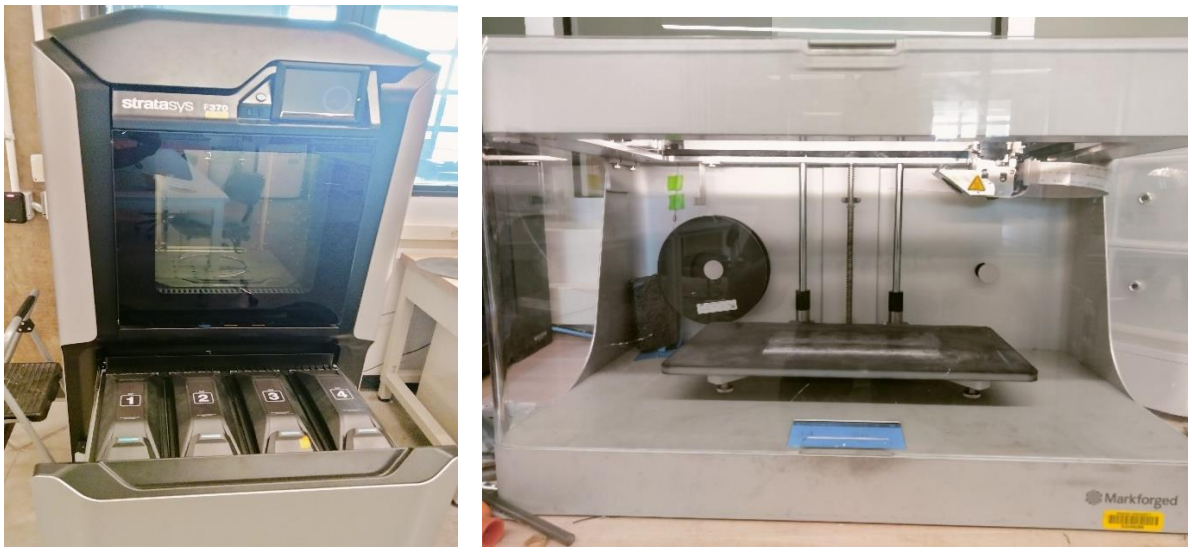

Figure 2.3: Images of the Stratasys F370 with its filament chamber and the Markforged MarkTwo.

2.1.2 Printing Software and Parameters

With each printer, a different software was needed to begin printing. First, a virtual CAD drawing of a part needs to be created through certain CAD software. Software like, AutoCAD, Solidworks, Creo Parametric, Siemens NX, and more. Once this CAD drawing is complete, a stereolithography or Standard tessellation language (.STL) file can be exported and is uploaded by the user and converted into a file that each printer reads. The name of the software that can read .STL files is a Slicer.

The first slicer that is used is Ultimaker's slicer, Cura. This slicer is very popular in the AM community due to its customizability. There are many parameters that this slicer allows the user to change, due to its open-source nature. This slicer was first created by David Braam and was then brough by Ultimaker and allows many personalized settings that the other slicers do not. Some of these parameters are: Print layer height, shell thickness, infill pattern, print temperature, build

plate temperature, and print speed. Even the filaments used can be changed from Ultimaker materials to general materials depending on the printer.

The second slicer is grabCAD Print. This slicer is used by Stratasys and for the F120 and F370 printers. This open-sourced slicer allows users to change a significantly lesser amount of parameters but allows customization for most of the important ones. This includes Infill amount, layer height, support print style, print scale and dimension. The print temperature is constant, relative to the chosen filament.

The final printing software that was used is MarkForged proprietary slicer, Eiger. This slicer is used to Within Eiger parameters like layer height, wall thickness, fiber and plastic layers can all be changed to fit the user's specifications. These fibers are printed at 235℃ and nylon is printed at 275℃. In this study, the geometry of the parts was modeled using the software SolidWorks®, exported as an .STL file and imported into Eiger™ for further modification. The specifications and printing parameters of each print are shown below in Table I. Preliminary test specimens were used with the two other printers for greater comfortability.

2.1.3 Carbon Nanotube Incorporation

There were two primary methods that were researched to incorporate short fibers within the filaments like Nylon and PLA – Dissolving/Extruding and Dry-mixing. The first method of dissolving the filaments took much effort. The primary dissolving agent were various acids that were known to dissolve nylon, namely formic acid and Benzene. Table 2.1 shows the reaction when nylon was submerged within each listed acid. Here, Nylon was placed in a beaker with the acid for 24hrs, while stirred and sometimes heated to facilitate dissolving. The acid with the greatest result was formic acid and will be henceforth used when explaining further methods of this process.

Table 2.1: The effect of certain acids with

Acid	**Reaction**
Benzene	Quickly dissolves nylon
Acetone	Partially dissolves with heat and time
Dimthylacetamide (DMA)	No reaction
Tetrahydrofuran	Dissolves nylon
Formic Acid	Quickly dissolve nylon
Dimethylformamide (DMF)	Dissolves nylon

After the nylon is dissolved, a weight percentage of CNT relative to the nylon will be placed and magnetically stirred. The weight percentages chosen were 1 wt.%, 3 wt.%, and 5 wt.%. Once the nanoreinforcement was evenly distributed, it was poured in a glass container under a fume hood and left for 24hrs to dry and another 24hrs in an oven at 75℃ to remove moisture. After this, the dried nylon would be cut into smaller pieces and placed in a single-screw extruder, the Filabot EX2 extruder. The cut nylon pieces would be fed into the extruder and melted at a temperature of 240℃ and the exiting strands of filament would be wound in Filabot's filament winder. However, when extruding the CNT-infused nylon, non-uniformity was experienced, and air bubbles were forming within the extruder and coming out of the die. So, another method was chosen.

This second method was infusing CNT with nylon through dry mixing the materials. Here, strands of nylon filament were cut and placed within a glass beaker with smaller weight percentages of CNT and stirred for more than an hour. It was found in literature that using more than 1 wt.% of nanoreinforcement lead to negligible increases in strength and unused material. Due to this, only two weight percentages were chosen, 0.1 wt.% and 0.3 wt.%. After stirring, the filaments were dried at 75℃ for 24hrs and used to print the compression, tensile and short beam shear test specimens. Images of non-reinforced vs reinforced samples can be shown in Figure 2.4.

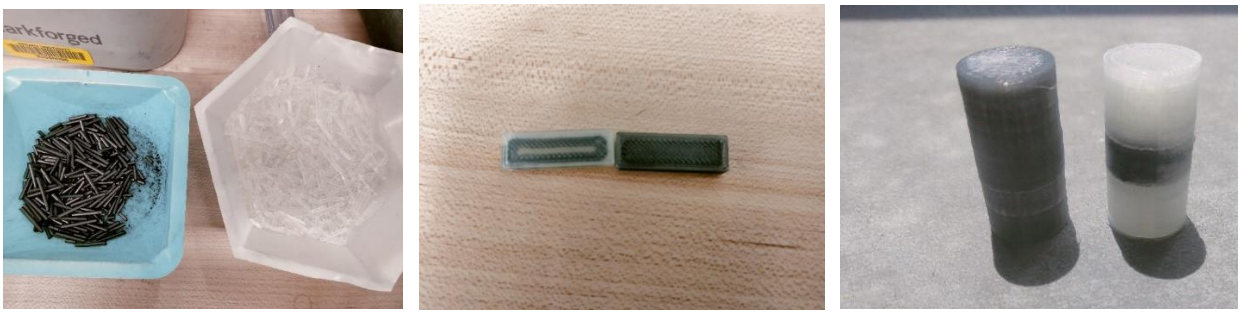

Figure 2.4: From left to right, image of pure nylon relative to CNT infused nylon filaments. Preliminary SBS test samples after first print. Final compression test specimens created in accordance to ASTM D695.

2.1.4 ASTM Standards and Preliminary Prints

For this project, in order to print uniform and replicable test specimens the American Society for Testing and Materials (ASTM) standards were used. These standards provide a baseline for various tests, but this project focused only on their mechanical tests and procedures. For the first procedure, the tensile tests, the ASTM D638 standard was used. This procedure is mainly used with reinforced and non-reinforced plastics and as Nylon is a thermoplastic this standard seemed the most applicable. Although F-42 is brought up concerning ASTM Standards, F-42 is just an ASTM governing committee for AM technologies, not a standard. Many in literature, doing similar mechanical tests, default to this standard [65, 69, 78] and produce replicable results.

When using the ASTM D638 standard, there are five different test specimens that one can create for testing. The differences between the five types are vast, ranging from differing thicknesses, gauge length, fillet radius and neck width. These can all be seen in Figure 2.5, taken from ASTM itself. For this project, a 3.2mm thick Type-1 test specimen was chosen due to its abundance use in literature and low material cost.

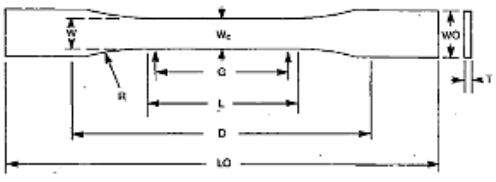

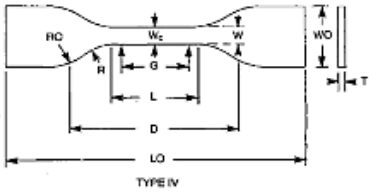

Specimen Dimensions for Thickness, *T*, mm (in.)[A]

Dimensions (see drawings)	7 (0.28) or under		Over 7 to 14 (0.28 to 0.55), incl	4 (0.16) or under		Tolerances
	Type I	Type II	Type III	Type IV[B]	Type V[C,D]	
W—Width of narrow section[E,F]	13 (0.50)	6 (0.25)	19 (0.75)	6 (0.25)	3.18 (0.125)	±0.5 (±0.02)[B,C]
L—Length of narrow section	57 (2.25)	57 (2.25)	57 (2.25)	33 (1.30)	9.53 (0.375)	±0.5 (±0.02)[C]
WO—Width overall, min[G]	19 (0.75)	19 (0.75)	29 (1.13)	19 (0.75)	...	+ 6.4 (+ 0.25)
WO—Width overall, min[G]	...	...	...	...	9.53 (0.375)	+ 3.18 (+ 0.125)
LO—Length overall, min[H,I]	165 (6.5)	183 (7.2)	246 (9.7)	115 (4.5)	63.5 (2.5)	no max (no max)
G—Gage length[I]	50 (2.00)	50 (2.00)	50 (2.00)	...	7.62 (0.300)	±0.25 (±0.010)[C]
G—Gage length[I]	...	...	...	25 (1.00)	...	±0.13 (±0.005)
D—Distance between grips	115 (4.5)	135 (5.3)	115 (4.5)	65 (2.5)[J]	25.4 (1.0)	±5 (±0.2)
R—Radius of fillet	76 (3.00)	76 (3.00)	76 (3.00)	14 (0.56)	12.7 (0.5)	±1 (±0.04)[C]
RO—Outer radius (Type IV)	...	...	...	25 (1.00)	...	±1 (±0.04)

Figure 2.5: Image of ASTM Types I, II, III, IV and V and each of their parameters and dimensions.

Another standard that is readily used is the ASTM D695 standard for compression testing. This standard is used to test the compressive strength of rigid plastics. Here, the standard dictates that a test sample could either have a circular, square or rectangular cross section and a circular one was chosen. To comply, a FDM printed specimen was to be printed with a diameter of 12.7mm or .5in and a height of 25.4mm and tested. The images of the ASTM D638-Type1 and D695 can be shown below in Figure 2.6.

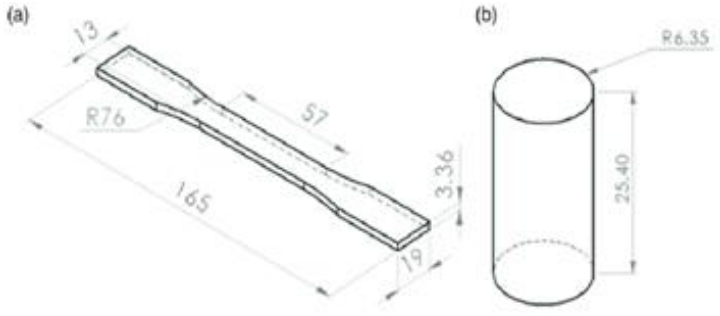

Figure 2.6: Schematic and dimensional representation of an ASTM D638-Type1 and D695 test specimen.

The final standard that was used is the ASTM D790 standard for testing the flexural strength of unreinforced and reinforced plastics, which is ideal for this test project. Here, the specimen was created with a rectangular cross section with dimensions of 62.5mm by 12.7mm by 3.2mm. The length was halved from the typical 125mm to conserve time and limited materials at the time, while producing accurate results.

After the standards were chosen, three printers were used to produce preliminary specimens, the Ultimaker3, Stratasys F120 & F370. These printers all have different advantages and disadvantages using a myriad of different filaments, nozzles and printing parameters.

The first printer used was the Ultimaker3, and it was this printer is by far the most user customizable printer, in terms of print parameters and usable filaments. The Ultimaker3 was created by the company Ultimaker in 2016 and is noted for its heated glass bed, dual extruders, large print area and diverse user settings. The Ultimaker and its line of 3d-printers all use the slicing software Cura. Cura is an opensource slicing software that was created by David Braam in 2008 before he was hired on by Ultimaker. Within Cura, a user can choose a preselected print settings chosen by the computer or dive in to more in-depth settings for greater control. Many of the options and modifications a user can choose can affect the final print and its properties, creating nearly limitless possibilities. The main parameters users tend to change are bed temperature, print and travel speed, extrusion rate, print temperature, Infill thickness, print layer height, travel speed, and even the fan speed. These settings can even change depending on the filaments used during the print. As stated earlier, the Ultimaker3 is able to print with nearly a dozen different materials and has two nozzles, a regular nozzle, named AA, that prints generic thermoplastics. The second nozzle, BB, only prints the support material, PVA but both nozzles can be coded to print at different temperatures and speeds. Figure 2.7 further displays the variety of a Cura’s options.

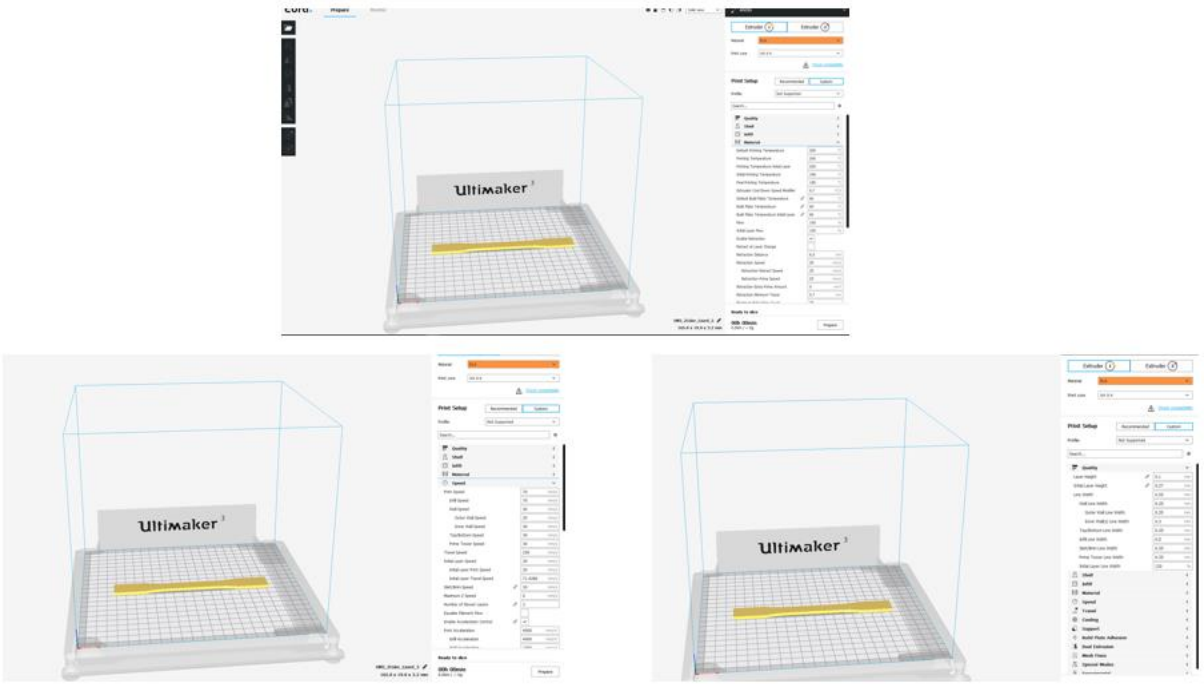

Figure 2.7: Screenshots of Cura 3.6 slicing parameters, namely: Speed, Quality and Material.

The second manufacturer that was used was Stratasys and its F-series printers. The first printer used was the F-120, a small industrial printer that prints ABS and SR-30 with its primary and support nozzles respectively. This printer is able to print ASA and ABS, but the latter is primarily used. The second printer is the F-370, which has a much larger print bed, filament variety and a separate filament holder within the printer. The F-370 prints with the same 0.4 nozzles, however these nozzles can be replaced to accommodate for different materials like TPU. This printer uses GrabCAD Print as its slicer and allows the user to change certain important settings but not nearly as much as Cura does. These settings also depend on the printer used, as GrabCAD Print allows the F-370 a few more changes than the F-120, especially when it comes to the infill density and layer heights.

Although, not much knowledge of 3d-printing is needed to print with the F-series printers, the Markforged MarkTwo takes the cake for being the most user-friendly of the three printing companies. With this dual nozzle printer, a plastic/Nylon nozzle of 0.4mm is used to print thermoplastics like Nylon, PLA, TPU and ULTEM 9085, with a fiber nozzle that prints continuous fibers like fiberglass, carbon and glass fiber. For a continuous curve, the Marktwo continuous fiber

nozzle can only print within a minimum width of 2.9mm. The minimum width for a projecting feature is 3.8mm so vertical prints are limited. In other projects and with other printers, it is possible to print a tensile, compression or SBS test sample on its side (upright along the z-axis), however, this is not possible for this project due to these size restrictions given by Markforged themselves.

Although this technology may be new, there is not a steep learning curve and this can be shown by how simple it is to use Markforged's proprietary slicer, Eiger. With this slicer, the user can upload their .STL drawing, determine how many layers of reinforcement they want and print one or multiple samples. However, due to this ease of use, there are many settings and parameters one cannot change or even find. This is offset by the novelty of the technology and there continues to be updates to the slicer, offering more customization. Table 2.2 below shows the various printers and their specifications.

Table 2.2: Specifications of each 3d-printer

	Ultimaker3	Stratasys F120	Stratasys F370	MarkForged Marktwo
Filaments	PLA, ABS, TPU, Nylon, PETG	ABS, ASA	PLA, ABS, ASA, TPU	Nylon, Onyx,
Support	PVA	SR-30	QSR	N/A
Nozzle(s)	AA: 0.25, 0.4, 0.8mm BB: 0.4, 0.	Primary: 0.4mm Support: 0.4mm	Primary: 0.4mm Support: 0.4mm	Primary: 0.4mm Fiber: 0.9mm
Slicer	Cura	GrabCAD Print	GrabCAD Print	Eiger

To first understand 3d-printing in the beginning of this project, the Ultimaker3 was available and previously used in our lab for previous testing. This printer proved to be vital in increasing my knowledge of 3d-printing and the FDM process. As stated before, Cura has many, many parameters that a user can change and determining the most influential parameters was top priority. The first parameter that was tested was melt and bed temperature and the material that was chosen for testing was PLA due to its ease of use and abundance. Because of the Ultimaker's glass bed, if heated too high the print will burn and fail, but if heated too low the print will not stick to the bed, so a delicate balance had to be found. The melting temperature was optimized to 200℃, with a bed temperature of 60℃ to print good parts.

The second parameter that was tested was layer height. It is well documented that layer height significantly impacts the mechanical properties of a print, with smaller layer heights generally being weaker and more time-consuming than prints with more considerable layer heights. Despite this, many still use a smaller layer height to increase the resolution and attractiveness of the print versus the rougher, more extensive layers. After testing, it was found that a layer height of .27mm, with a layer width of .35mm was able to produce strong, fast and visually pleasing prints.

The final parameter that was tested was infill density. This was arguably the most critical parameter, as this directly affected how much material and time every print would take. The infill pattern was first tested, and only minor changes in the maximum load amount could be found. The infill patterns that showed the greatest tensile test were line, grid, and of course, solid fill. Line and grid patterns used less material than solid infill, with grid pattern and line pattern prints taking less and more time than solid infill, respectively. For example, a tensile specimen printed to 100% infill would take 3hrs and 7min, while a print that was 90% infill took 2hrs and 9mins, and 80% taking 2hrs and 7min.

Although the amount of time can drastically change, the amount of material does not experience such a significant change itself. Because of this, preliminary test samples of both ABS and PLA printed from the Ultimaker3 and Stratasys printers of various infill amounts were tested for their tensile strength. It was found that solid fill (100% infill) was the strongest, with the other percentages lagging far behind. Due to this, solid fill was used for preliminary testing for all three standards, and when used experimentally, the continuously reinforced prints were coded within Eiger for solid (100%) infill. Figure 2.8 shows the tensile samples of various infill amounts after testing.

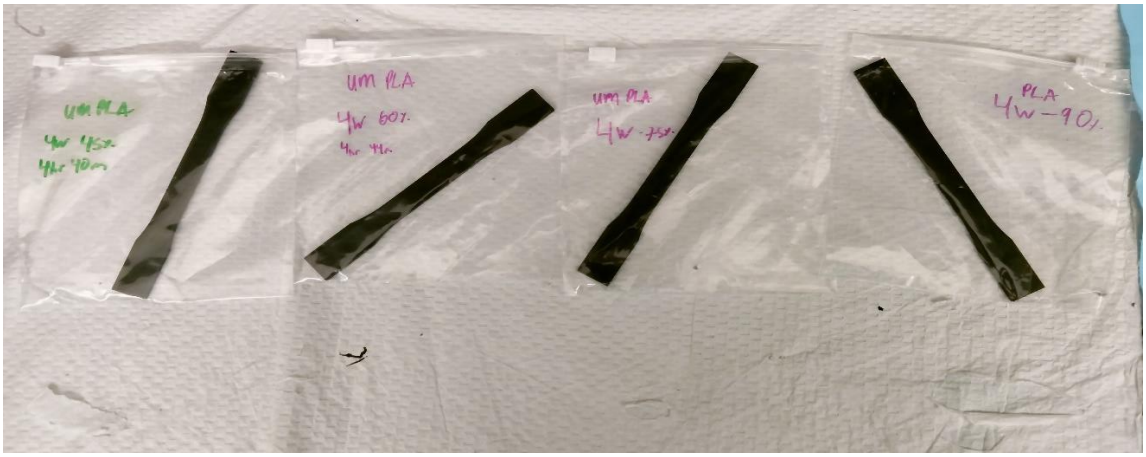

Figure 2.8: PLA tensile test coupons at 45%, 60%, 75%, and 90% infill

2.2 Mechanical Strength

To test these materials, various testing machines were used to determine and validate the maximum force of each material. The first of these machines is the Jinan Focus Test 5kN Universal testing Machine (UTM), model WDW-5. This 5kN UTM machine tested three primary testing methods, tensile, compression, and short beam shear. Because of this, it was beneficial for this project. Figure 2.9 below shows the UTM Machine primed and ready for tensile, compression, and SBS testing.

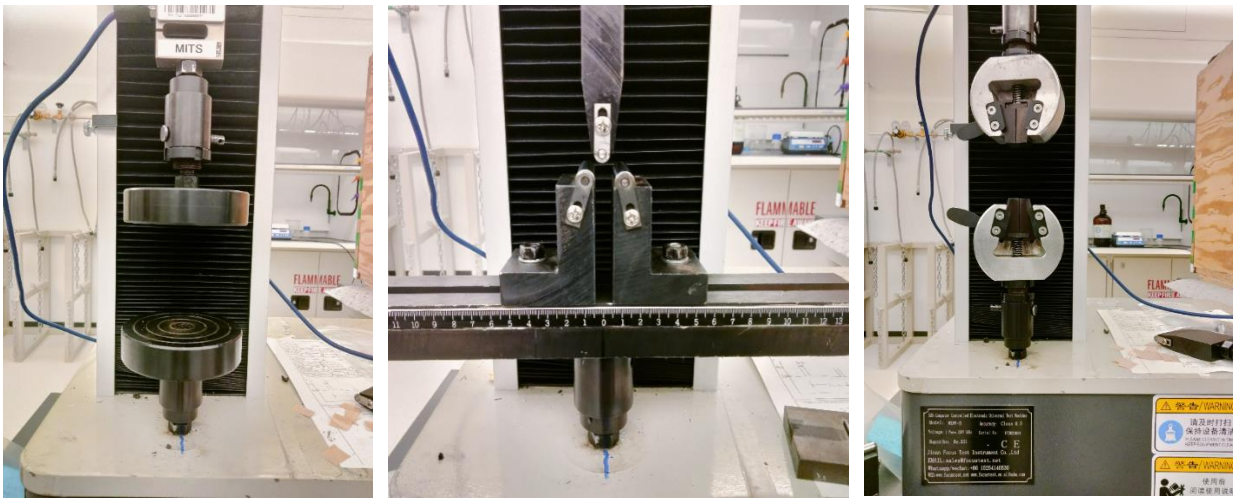

Figure 2.9: From left to right, images of the UTM Machine unloaded and ready for compression, SBS, and tensile testing.

However, because this UTM machine could only test up to 5kN, it could not test the carbon fiber compression or tensile samples without overloading itself. This next machine solved this problem as it could test with up to 300kN of force. A 300kN MarxTest manufactured electric universal testing machine was used with a TAIQIN TQ-1A 300Kn sensor. Despite the ability to test up to 300kN, the heads could be replaced so that if a user wants to test at only 20kN or lower, they can. This was done, and to test deformation, a YSJ50-10 strain gauge was used when completing a test and can be seen in the loading screen. On this screen, when a tensile test is conducted, the material data is uploaded on the computer screen and updated with the machine 15 times every second. Various parameters could then be graphed in that visual display. The key parameters researched are load vs. displacement, load vs. strain, and stress vs strain. For this project, load vs. displacement took special precedence, as the other parameters will be more critical in future projects. Images of this machine can be seen below, along with a screenshot of this UTM's visual display.

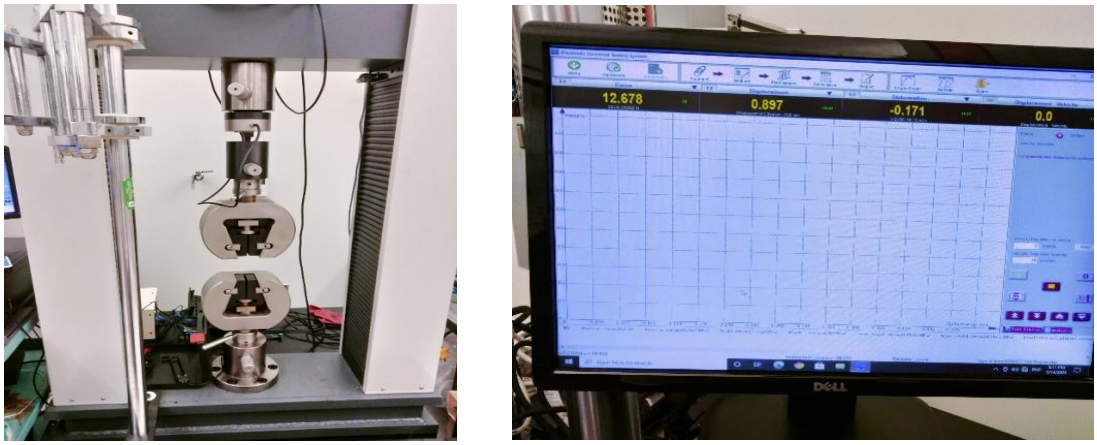

Figure 2.10: Setup of the MarxTest UTM machine and visual representation of the graph

To determine the micro and macrostructure of the prints, a Scanning Electron Microscope, or SEM, machine was used to view the test specimens before and after testing. In this project, the JSM-7800 field emission scanning electron microscope was used for image analysis, viewing the specimens at a pressure of 3.6e-4 bar. Before SEM observation, a thin layer of gold coating was placed to avoid the electrical charging of each specimen.

3. FINITE ELEMENT ANALYSIS

3.1 Introduction

Finite element analysis is a numerical, analytical method that allows a user to apply conventional manufacturing and testing techniques on a beam, shell, or solid all having one, two, and three dimensions, respectively. FEA allows users to predict and simulate the response of their material or part when placed under certain loading conditions. These conditions range from pure structural analysis, thermal effects, aerodynamic forces, and even typology optimization. This provides a unique opportunity for a user, company, or research group to experiment with failure conditions and optimize parameters before creating a physical part. However, there are some difficulties when using FEA with AM-created components.

Using by using FEA, shell elements of a CAD drawing can be incorporated into a composite layup. This can be done within SolidWorks, ANSYS, ABAQUS, and other FEA software packages. However, it has been shown that manufactured parts show inconsistencies when compared to simulated results. FDM slicers allow a printer to print in many complex forms, angles, and patterns, all to optimize speed, material usage, and print time, all things that are difficult to replicate using finite element analysis. The print path and curves that a printer can achieve are not replicable within FEA, so an approximation is used to produce similar results.

Another difficulty is accurately reproducing material properties. Most prints are printed with one nozzle and thermoplastic, all with the same properties and can be easily tested. However, there are printers that can print with two different materials, and estimating the interaction between the two are even more complicated than a consistent print. This gets even more trickier to simulate if the second material is continuous reinforcement (orthotropic) for the first material (isotropic), like a composite similar to carbon fiber prepregs. Bluntly, modeling a continuously reinforced material produced through additive manufacturing as an isotropic material is impossible. The orthotropic nature of fiber reinforcement disallows such a case as the material properties of the fiber can be changed based on its angle/orientation. Isotropic materials have the same properties regardless of

direction, so combining both was a challenge for FEA software. To solve this issue, a shell is typically used to create a part layer by layer, incredibly similar to FDM, only virtual.

3.2 FEA Parameters

In this project, modeling a completely homogeneous material would not be accurate nor portray the FDM process correctly. To rectify this, it is much better to simulate the material layer by layer or shell by shell, each with changeable materials and angles. Then combine these materials all into one part, ready for testing. This process can be done using a toolkit within ANSYS called ACP-pre/post.

Here, the chosen material properties were found both in literature and commercially by MarkForged themselves. The material properties for Markforged carbon fiber and nylon were found. However, only the isotropic properties and strength were given. This is not a problem for Nylon, however the orthotropic properties needed to be researched. Because of this, two different papers gave two different properties, so determining which was better for this test was paramount. Both CF properties were placed as “AS4 Yarn” and “Estimated CF” properties and tested versus experimental results. Images of the material properties can be seen in Figure 3.1. After this, a CAD drawing of an ASTM D638 was created and uploaded as a shell model, having only length and width. Meshing was next, and it is well known that the results generated using ANSYS and especially ACP-Pre are sensitive to the size of the mesh ANSYS generates. So, for this project, instead of the computer-generated mesh size of 3.1mm, a size of 1.74mm per node was chosen and the change in the final results was noticeable. Then the mesh was uploaded into ACP-Pre.

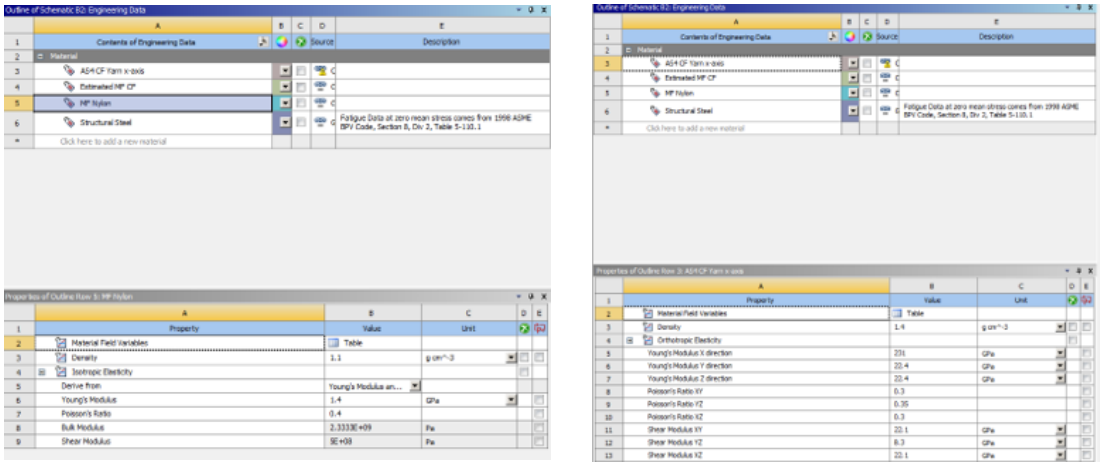

Figure 3.1: Displays of the ANSYS Material Properties and Values for Markforged's Nylon and AS4 carbon fiber.

3.3 ACP-Pre

Once ACP Pre is open, the first thing one should do is select the materials they wish to use. As stated before, only three were used (outside of the default structural steel) Nylon white, AS4 yarn and Estimated CF. After this, a fabric of the material was created. This specified the thickness of each material layer (0.125mm for both CF and nylon), and its price per area can be inputted there. After this, the stackup of each material could be placed, named and assigned. Under this parameter, a user can determine what fabric/material they want to use to create a stackup and then place the angle of each fabric layer and its symmetry. Multiple stackups can be created with a nearly infinite variance between them. Figure 3.2 shows the stackup that was used to create a tensile test specimen that had 16 layers of CF reinforcement. After this, the user can create a ply, a combination of various stackups, and determine how they want to use that as well. Figure 3.2 also shows the creation of the ply that was tested.

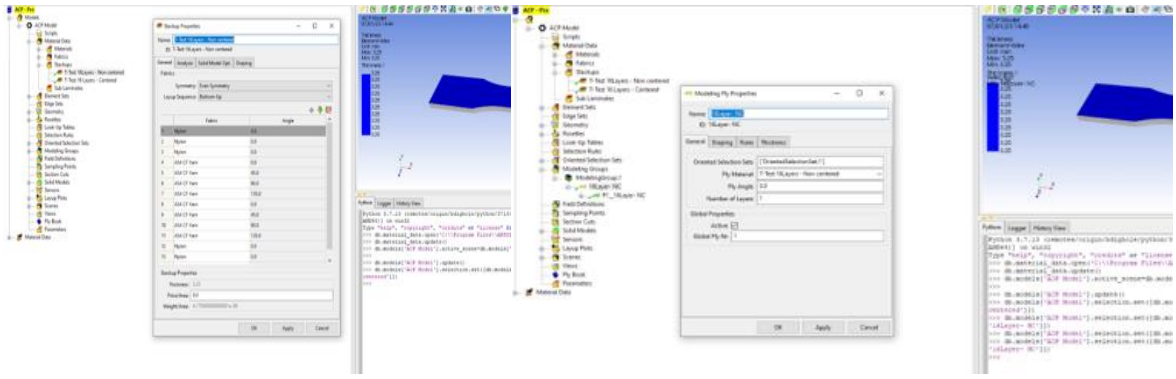

Figure 3.2: Visual representation of the software ACP-Pre and the parameters inserted and used.

Finally, once the part is accurately modeled in ACP, with the correct angles, symmetry, thickness and materials, it is ready for testing. In this project, the workbench tool Static Structural was used to determine the structural and mechanical properties of the test specimen. A fixed support and load/force could be applied to the part. Because the tensile test specimen was converted into a shell and not a solid, when trying to simulate the fixed supports made by a tensile machine's grips, the software would not register it. To get reasonable results, a fixed support was only placed at the bottom of the specimen, not the uniform section before the specimen's neck/gauge. This can be seen in Figure 3.3.

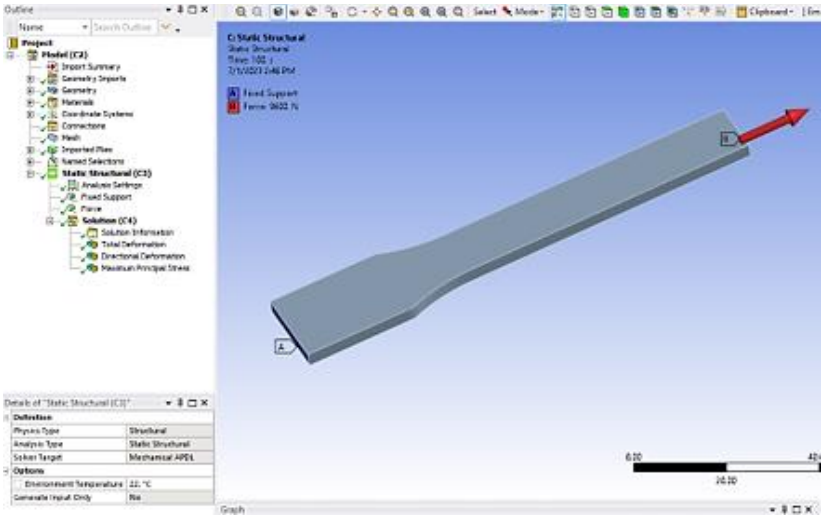

Figure 3.3: View of the testing parameters used for testing

Once the fixed support was placed, a force was placed at the end of the neck and given values that were the same as the maximum values that the experimental test specimen experienced and the solutions were found. The solutions that were looked for were: total deformation, directional deformation and the Maximum principal stress.

After this, a total of six workbench modules were created to simulate the six experimental samples that were tested. The first is a tensile specimen of 26 layers consisting of three layers of nylon, eight layers of carbon fiber, four more layers of nylon, another eight layers of carbon fiber and finally, three layers of nylon. This formation was called 16 Carbon Fiber-not centered or 16CF-NC due to the carbon fiber being split in the middle with layers of nylon. The second formation consisted of five layers of nylon with 16 layers of carbon fiber, ending with five layers of nylon. This formation was called 16CF-Centered. The remaining four experimental samples followed these two formations and were 12CF-NC, 12CF-Centered, 8CF-NC, and 8CF-Centered. A screenshot of all six workbenches and the first two formations, can be shown in Figure 3.4. Finally, compression tests were also simulated in ANSYS. They followed the same methodology, but the verification of the results could not be performed experimentally due to lack of materials, like a strain gauge.

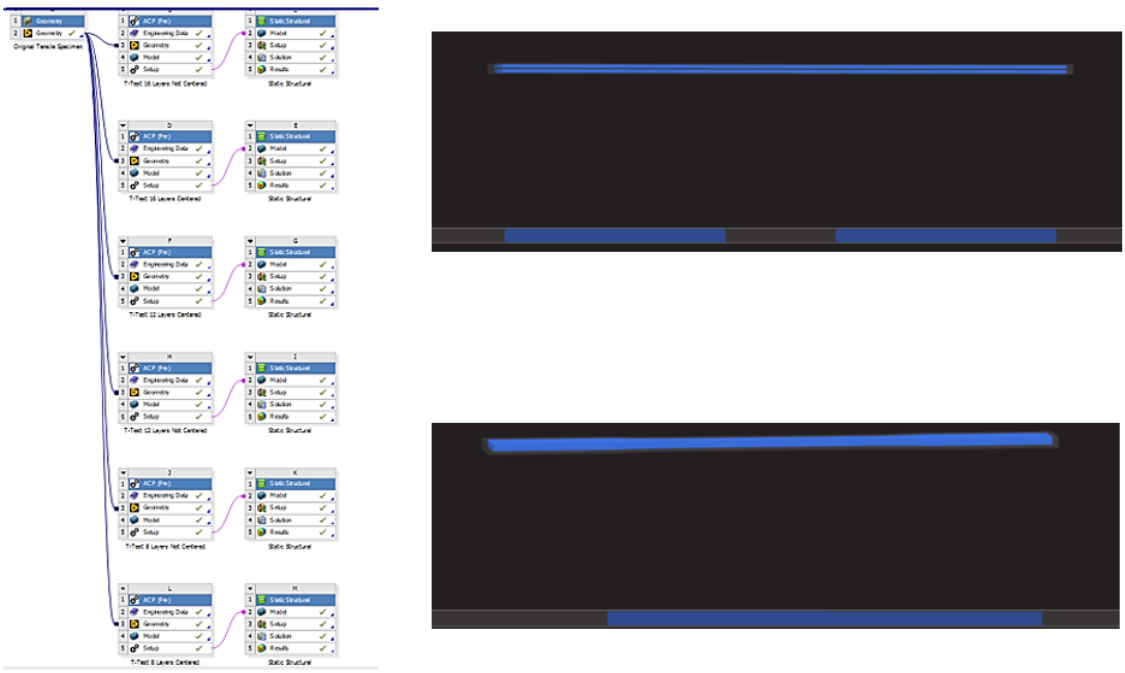

Figure 3.4: Image of the completely compiled ANSYS Workbench with all 6 test samples. As well as a visual representation of Non-centered (NC) vs Centered samples look like.

Finally, as stated before, when using ANSYS, a considerable number of assumptions were made. ANSYS Static Structural assumes linearly elastic behavior. Also, the assumed material properties taken from literature and MarkForged can vary due to material storage, handling, and usage. Another assumption is the isotropic nature of the fibers and perfect adhesion between the fiber and nylon matrix. As will be shown later, when layers of nylon and fiber are printed, the adhesion between the transition layers is not perfect as assumed in ANSYS, which can lead to margins of error between the two.

4. RESULTS AND DISCUSSION

4.1 Microstructural Analysis

As stated before, material characterization is essential in understanding the part that nanomaterials play in mechanical reinforcement. Although the darkening of the nylon filaments and prints indicated the presence of nanoreinforcement, microstructural analysis was necessary to determine the presence and effect of CNTs within each part. So certain test specimens, namely tensile test samples, were subject to SEM imaging to delve deeper. The camera was focused on the intersection of nylon and carbon fiber layers, as the composite test samples' microstructural morphology and failure mechanisms can be observed there. It can be seen in Figure 4.1 that within this nylon-carbon fiber intersection, ribbon-like carbon fiber nanotube films were found. This is supported by literature to represent the form of impregnated CNTs when adhesion takes place.

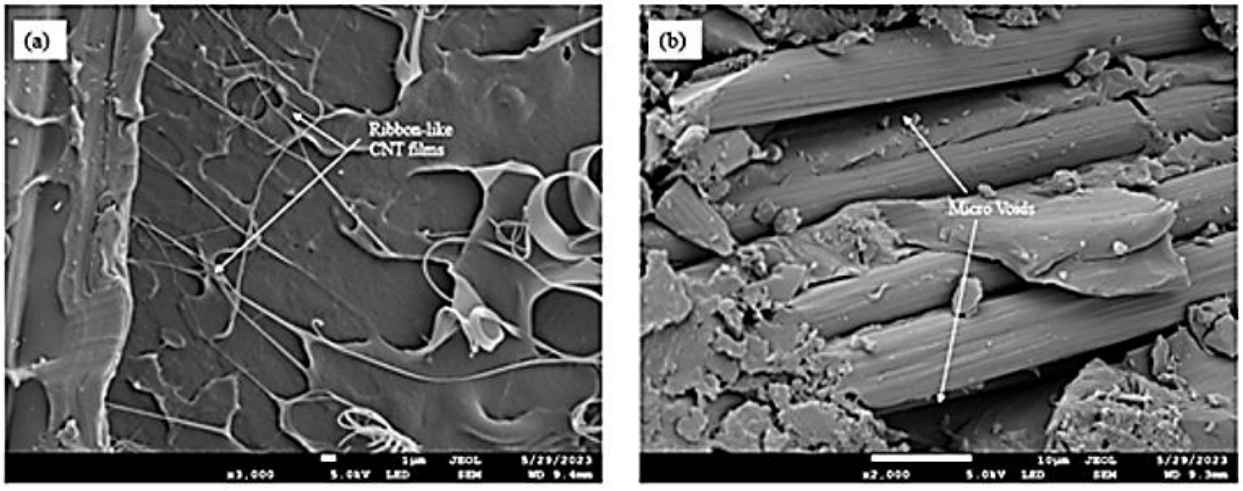

Figure 4.1: SEM Images of a). Coiled CNT formations within Nylon substrates, and b). Micro-void formation within failure samples

These nanoribbons lead to a decreased influence of matrix debonding and fiber breakage. Post-fracture analysis shows the formation of micro-voids, leading to fiber breakage. This is due to crack nucleation sites at the transition layers from nylon to carbon fiber and vice versa. As stated before, ANSYS does not replicate this, but these micro-voids reduce adhesion between the transition layers. The crack nucleation sites grow and propagate to ultimately lead to delamination.

4.2 Experimental Results

4.2.1 Tensile Testing

The first and most important tests that were conducted were the tensile tests. According to ASTM Standards, at least five samples are needed to thoroughly verify one's findings, so two pure nylon sample types were printed, centered and non-centered, as well as 0.1wt% CNT samples. As stated before, the 300kN UTM machine with 20kN grips were used to test the samples. It should also be known that these samples were formed as non-centered samples. The first test showed the maximum loads 0.1wt% CNT vs nylon, when compared there was a decrease of less than 5%, or around 450N when CNT was incorporated into nylon, see Figure 4.2. Also, when multiple samples were tested, CNT-reinforced nylon was also less strong on average compared to pure nylon also see in Table 4.1. This can be due to the vast presence of carbon fiber relative to reinforced and non-reinforced nylon, generating a much larger volume fraction of carbon fiber. The printing time of these samples are also much longer than the two other test specimens so that may have influenced the material properties again.

Table 4.1: Tabulated representation of the found average and max load values for tensile tests.

	Average	Maximum
Tensile - Nylon	8602N	9786N
Tensile – 0.1% CNT	8557N	9341N

The second set of tests were determining the effects of centered versus non-centered tensile specimens. The samples for this test were only made of nylon and were not nanoreinforced. A significant change in the maximum amount of load each sample can reach was discovered, as centered samples reached only 7420N, compared to 9786N the non-centered samples reached. The reason for these differences could be due to the increased distribution the carbon fiber has when non centered.

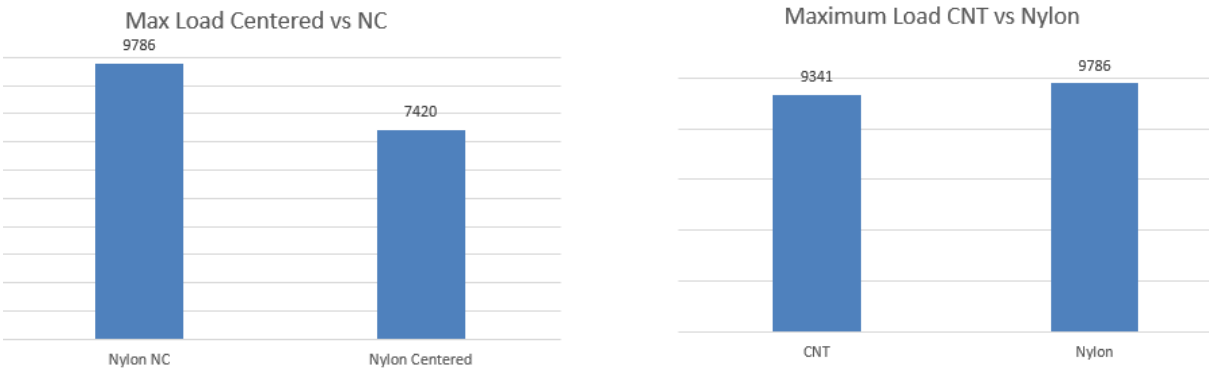

Figure 4.2: Graphical representation of the maximum loads each test sample experienced, measured in Newtons.

4.2.2 SBS Testing

To determine the flexural properties of reinforced vs non-reinforced nylon, after testing the data for both samples were analyzed. It was revealed that the short beam strength of the samples showed greater increases of strength when tested. The maximum amount of force the samples could withstand were 787N and 868N for pure and CNT-reinforced Nylon. When multiple samples were tested, the average maximum force of pure nylon was 690N with CNT-reinforced Nylon showing results of 749N, an increase of 8.6%. Also, statistically, the standard deviation (SD) was also tested and showed that reinforced nylon displayed a lower SD at 108N than pure nylon's 204N. Showing that as well as increasing the strength of nylon, CNT can also create more consistent results, which can be summarized in Table 4.2.

Table 4.2: Tabulated representation of the found average and max load values and the standard deviation from short beam shear tests.

	Average	Maximum	Deviation
SBS – Nylon	690N	787N	204N
SBS – 0.1% CNT	749N	868N	108N

4.2.3 Compression Testing

The final test that was conducted was the compression test and the results were also analyzed. Here, five or more samples of reinforced and unreinforced nylon were loaded into the UTM and tested, and surprisingly, compression samples showed the most significant increase in mechanical strength. The maximum force pure nylon could withstand before failure was 2398N, and the maximum for CNT reinforced Nylon reached 2610N, an increase of nearly 9%. The average force these samples could withstand increased from 1970N to 2398N, growing more than 20%. Statistically, it could also be seen that the standard deviation decreased from 390N to 255N. These results can be seen tabulated in Table 4.3. Figure 4.5 also shows the increases in maximum force and average force graphically.

Table 4.3: Tabulated representation of the found average and max load values and the standard deviation from compression tests.

	Average	Maximum	Deviation
Compression - Nylon	1970N	2398N	390N
Compression - 0.1% CNT	2393N	2610N	255N

4.3 Simulated Results

As stated before, tensile test coupons were modeled on SolidWorks according to ASTM D638 standards and printed as Type 1 test samples. It was then simulated and tested in ANSYS and compared with experimental results for variability.

4.3.1 Non-Centered Tensile Results

Simulated tensile tests can provide strong a strong correlation with experimental results. However, due to not having sufficient material properties for nanoreinforced nylon, modeling was only limited to pure Nylon samples. A fixed support was placed in the base of the sample, and a load was placed at the neck of the sample to replicate experimental parameters. The three solution parameters that was looked for were total deformation, directional deformation, and maximum principal stress.

The first sample that was tested was the 16 layered-NC nylon sample. Here, a load of 9600N was placed as the load, and it was discovered that a deformation of .425mm was exhibited and a maximum principal stress of 652 MPa was exhibited. The next sample that was tested was 12CL-NC and that was placed under a load of 7400N. Under that load, a deformation of .417mm was also experienced and a max stress of 611MPa. Finally, the last test sample that was simulated was 8CL-NC and placed under a load of 4600N. Here, a deformation of .429mm was found with a max stress of 601MPa. Figures of the maximum principal stress and deformation can be shown in Figures 4.3 and 4.4.

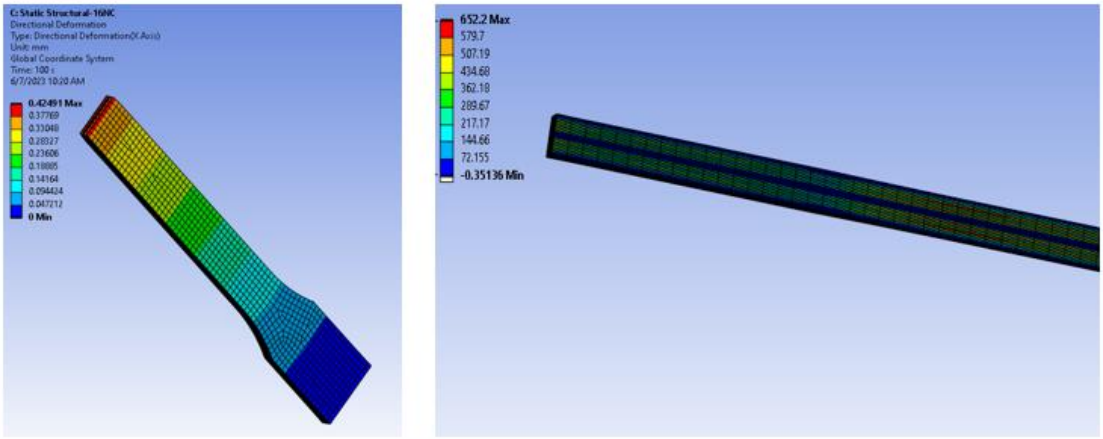

Figure 4.3: Simulated representation of the total deformation and Maximum principal stress experienced by 16CF-NC test specimens.

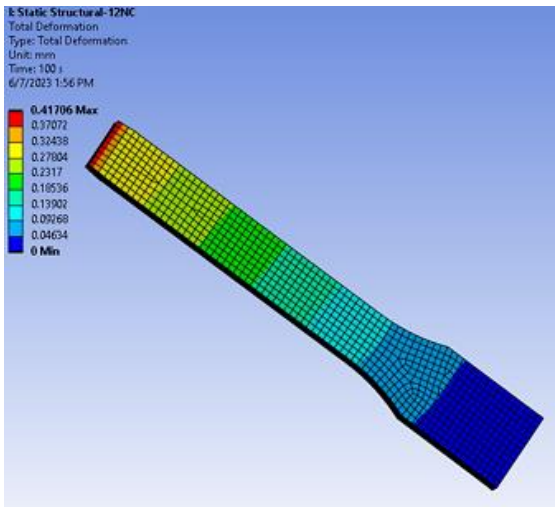

Figure 4.4: Simulated representation of the total deformation experienced by 12CF-NC test specimens.

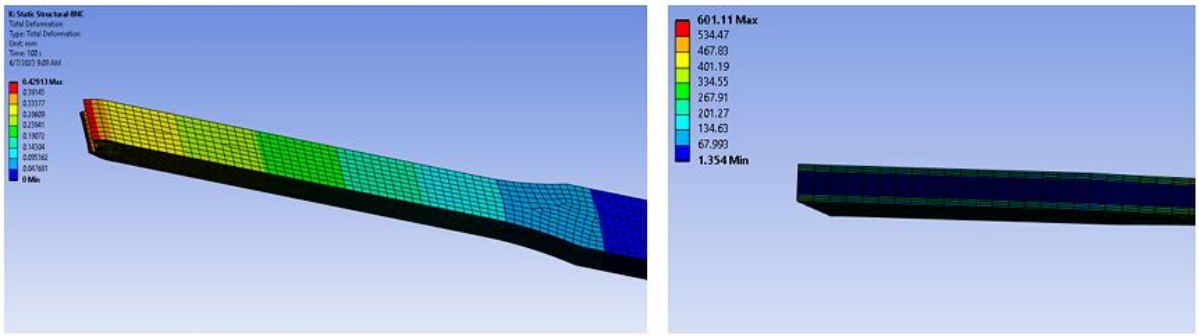

Figure 4.5: Simulated representation of the total deformation and Maximum principal stress experienced by 8CF-NC test specimens.

4.3.2 Centered Tensile Results

16CF-centered, 12CF-centered and 8CF-centered were all tested with the same load conditions for the same parameters. It was shown that centered samples had larger deformations/elongations relative to non-centered samples. Here, 16CF-centered experienced a deformation of .483mm and a max principal stress of 645MPa under the same load of 9600N and is shown in Figure 4.5. The 12CF-Centered sample was also placed under a load of 9600N and experienced a max stress of 804MPa. Finally, the last test sample, 8CF-NC was tested at 4600N and showed a Maximum principle stress of 601 MPa. These simulated results can be seen in Figures 4.6 and 4.7 respectively.

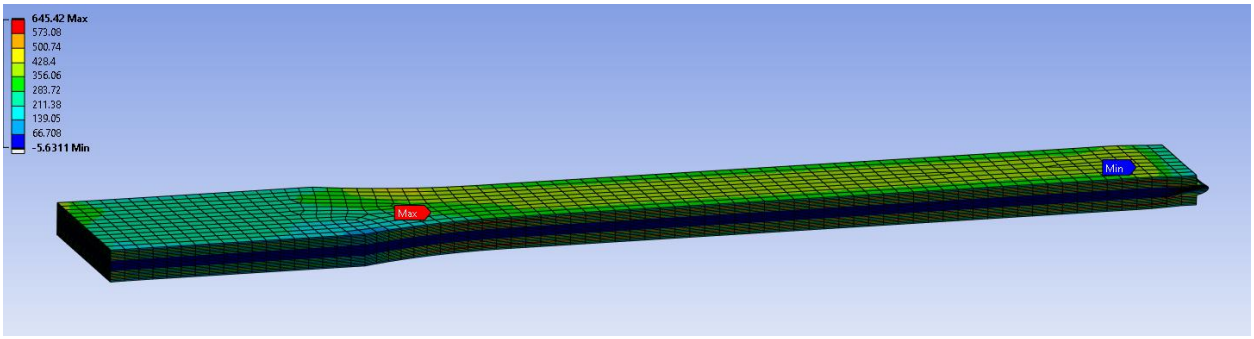

Figure 4.6: Maximum Principal Stress Simulation Results for 16CF-Centered Test Specimen

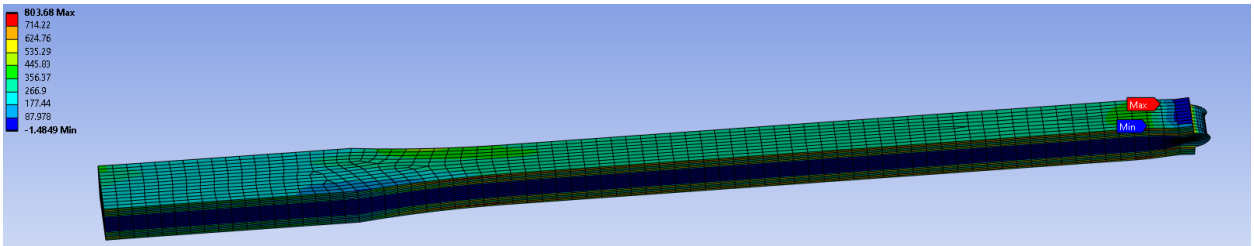

Figure 4.7: Maximum Principal Stress Simulation Results for 12CF-Centered Test Specimen

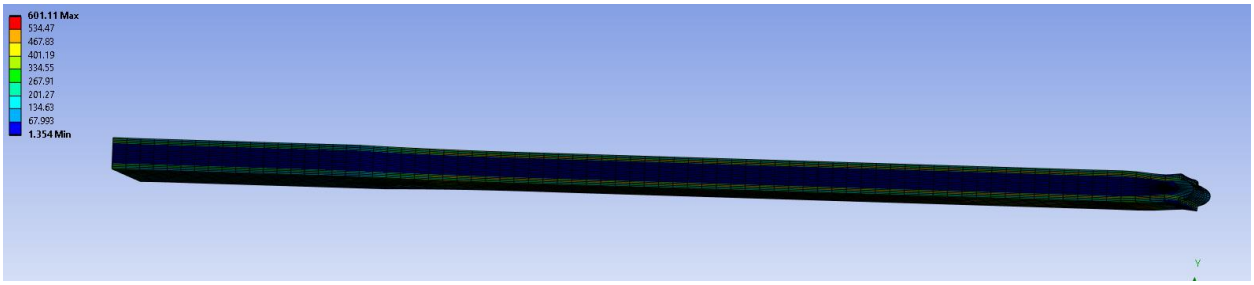

Figure 4.8: Maximum Principal Stress Simulation Results for 8CF-Centered Test Specimen

These results further reinforcing experimental values and the earlier hypothesis that carbon fiber centered samples would produce weaker materials than non-centered tensile samples. From these values, it would seem as though the maximum deformation that a tensile sample can withstand is around .42 to .43mm, before failure. This was not the case experimentally. When compared with experimental results, there were some deviations compared the modeled samples, which will be further explained.

Finally, it was determined that the three centered samples were not to be compared with experimental results, although they may provide differing results. This was primarily due to time constraints as additional test specimens were to be created to fit the ASTM standards and conduct accurate statistical analysis.

4.3.3 Compression Tests

Initially, compression tests were to be explored experimentally and modeled in ANSYS but as stated before, the lack of measuring instruments hindered achieving this. Nevertheless, sample compression test specimens were modeled and tested for feasibility. Figure 4.9 shows the ANSYS

results for total deformation and maximum stress. A fixed support was placed at the bottom of the sample and a load of 2000N was placed on the sample which deformed the sample .13mm. It should also be noted that the ply with the greatest failure cannot be found, however failure seems to occur within the last 50 layers of the print, which was also where failure occurred when experimental testing occurred.

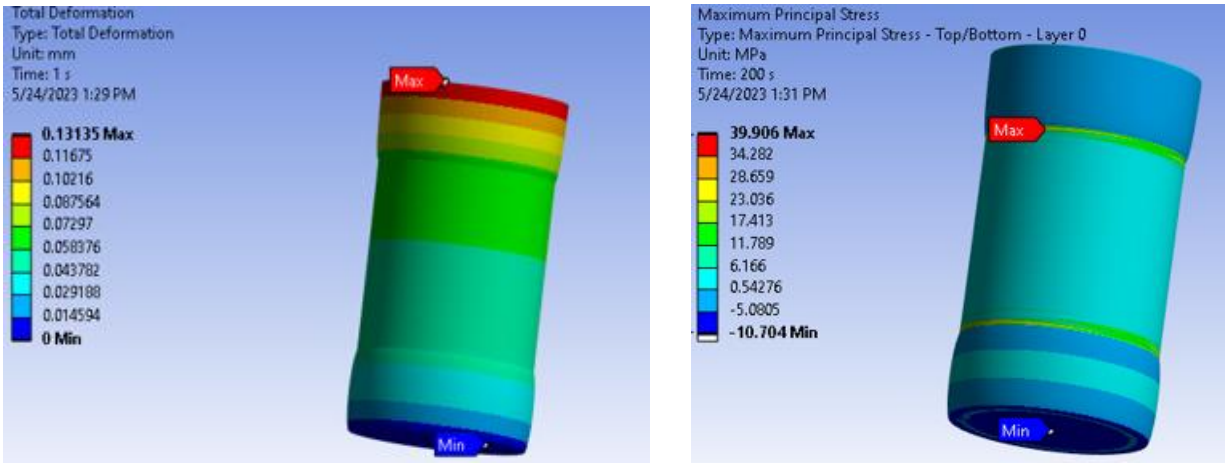

Figure 4.9: Results for compression Tests

4.4 Comparison of Results – Margins of Error

In this study, the goal of verifying the feasibility of using nanoreinforcement to increase mechanical properties was fulfilled. However, a secondary goal was to determine how accurate and precise FEA and simulated results could be compared with experimental results. As stated before, certain assumptions were used when replicating this project virtually in ACP-Pre. However, in general, the data comparison of experimental and simulated results was nearly equivalent with each other.

First, the deformation between 16CF-NC was compared. It can be seen that .54mm of deformation was experienced when tested in the UTM machine, and ANSYS states that a deformation of .425mm would be experienced when a load of 9600N is exerted. This produces a margin of error of 27.1%. The next sample was the 12CF-NC and a .5mm was found after testing, but ANSYS gave a deformation of .417mm, resulting in a margin of error of 19.8%. The final sample was the 8CF-NC and it produced a deformation of .407mm, compared to ANSYS' .454mm and giving a margin of error close to 10%. Table 4.4 displays these results below.

Table 4.4: Tabular representation of the margin of errors.

	Exp. deformation (mm)	Sim. deformation (mm)	Error
8 Layers CF	.407	.454	10.3%
12 Layers CF	.5	.417	19.8%
16 Layers CF	.54	.425	27.1%

It can be seen that the higher the amount of carbon fiber, the higher the margin of error seems to become. This could be due to carbon fiber's nonlinear properties once it approaches and ultimately reached failure, as opposed to Nylon's relatively linear properties. This could not be captured accurately in ANSYS, as it is much more difficult to simulate nonlinear properties than completely linear material properties.

There are a few reasons why there is a margin of error in the first place. The first reason was described earlier, the variance between linear and nonlinear properties. The second reason for this margin of error could be due to Nylon's hygroscopic nature absorbing water from the atmosphere. This is well known to decrease the print quality and mechanical strength of nylon and was prone to do so earlier in this project. It should also be noted that the nylon that was used for the majority of this project is "Nylon EOL" while the material properties that was used in ANSYS was from "Tough Nylon" as nylon EOL's material properties were not found. Another reason could be due to ANSYS assuming perfect adhesion between each print layer. Which has been shown to not be the case, especially between transition layers. Machine error between the UTM and sensor could also be cause of error. It is also possible that any combination of these reasons could have affected the results, leading to margins of error.

4.5 Summary and Conclusion

FDM has grown explosively in the past few decades, and it is abundantly clear that many are interested in its capabilities. One way that people have been pushing the limits of 3d-printing is through the use of nanomaterials. Researchers all over the world have explored incorporating various types of nanofillers like CNT, CNF, GO, Graphene and Graphite into filaments. However, there has been little research for incorporating both nano/short fiber reinforcement with continuous

fiber. In this study, by using the MarkForged Marktwo printer, it is possible to print continuous fibers and it has been shown that there is great potential for this.

This can be shown namely with the significant increases in mechanical strength that has been observed when using these nanoreinforcements. However, to verify these results preliminary testing was conducted using the Ultimaker3 & Stratasys printers. These printers printed initial test samples according to ASTM standards using PLA and ABS respectively. It was shown that Infill amount, print speed, temperature and layer height are incredibly important for print quality. These two printers are able to print multiple materials, however only the Marktwo can naturally print continuous and short fibers. The Ultimaker has the potential to print continuous fibers due to Cura's incredible flexibility and by purchasing nozzles that can print continuous fibers, however this is seldom explored.

When preliminary testing was completed, then came incorporating carbon fiber into the filaments that would be used. After trying many acids, dissolving & extruding CNT-infused nylon was shown to be ineffective. The other alternative was to dry mix the nanomaterials and this proved to be much more successful. However, this method is limited to small weight percentages and increasing it being explored.

Testing of pure and nano-reinforced nylon was conducted using universal testing machines. Here, increases of up to 20% can be shown when 0.1wt% CNT is infused with nylon. Material properties generally increased, with a negligible difference in tensile properties, which is estimated to be due to the lack of Nylon within the printed materials.

FEA was then used to simulate and replicate experimental findings. This was done by using ANSYS-ACP to provide accurate results and duplicate the AM process of additively adding layer of nylon and carbon fiber continuously. The material properties were taken from Markforged and other researchers in literature. Six carbon fiber tensile samples were created used to test the effect that carbon fiber amount and layer sequence (centered vs. non-centered) had on the mechanical strength. Both compressive and tensile tests were replicated using the same forces applied to the

samples and tested for maximum principal stress, total and directional deformation. Due to various assumptions, the margin of error stayed within single and double digits.

4.6 Future Work

Having completed this phase of the project, now let us look at the different ways this project can progress even further. The first way to delve deeper is by examining ways to dissolve and extrude Nylon. This was difficult due to Nylon's hygroscopic nature, however there are ways that others were able to do so and with greater wt% of nanoreinforcements. A way to increase the weight percentage of CNTs during dry mixing would be another important research topic that could show great potential, as well as using different nanomaterials.

When it comes to using the printers, there is potential to use the Ultimaker & Cura to create prints with continuous reinforcement and customizable printing parameters. The Ulitmaker S5 and S7 have CC nozzles, that are able to print short fibers however, this is rarely explored. There are still ways to print with continuous fibers due to Cura's customizable print parameters and the S5 & S7's ability to print with other 3rd-party nozzles.

Another way to delve deeper and creating more accurate results is by using ANSYS to simulate nonlinear properties. Ansys ACP-Pre allows results to be calculated but it only assumes linear properties, unless otherwise inputted by the user. If the nonlinear properties of AS4-yarn could be inputted, this undoubtedly will create more accurate results and decrease error. Error could also be decreased by changing the printed material from nylon EOL to tough nylon, as tough nylon was the only nylon with material properties that could be found. Finally, obtaining more parameters such as maximum stress, Tsai-Hill failure criteria, and shear stress through ansys analysis would increase our understanding of each print's limits.

All of these will aim to complete this project's final goal of incorporating findings and prints in commercial applications – namely, the automotive industry. One way of doing so is by printing the rear bumper of a car piece by piece. By reinforcing nylon with various nanofillers and continuous fibers, the bumper can reach and possibly exceed the strength and durability of generic bumpers. Another goal would be creating multifunctional carbon fiber composites through

additive manufacturing. A few research labs have delved into creating multifunctional CFs, but none have looked at using additive manufacturing as a means of doing so.

This project has been able to increase our knowledge of additive manufacturing, specifically 3d-printing continuous and short carbon fibers. Much progress has been done and shown in this thesis and much more is still possible with this technology.

PUBLICATIONS

Publications:

1. Vidya Wable, Pias Kumar Biswas, Reza Moheimani, Nojan Aliahmad, **Peter Omole**, Amanda P. Siegel, Mangilal Agarwal, Hamid Dalir. Engineering the electrospinning of MWCNTs/epoxy nanofiber scaffolds to enhance physical and mechanical properties of CFRPs, Composites Science and Technology, Volume 213, 2021, 108941, ISSN 0266-3538, https://doi.org/10.1016/j.compscitech.2021.108941.
2. Pias Kumar Biswas, **Oluwaseun Omole**, Garrett Alan Peterson, Eric Cumbo, Hamid Dalir, Mangilal Agarwal. Nanofillers Reinforcement to Strengthen Carbon Fiber-Epoxy Composites: Processing, Characterizations, and Applications, https://doi.org/10.3389/fmats.2022.1089996.
3. **Oluwaseun Omole**, Pias Kumar Biswas, Landen Swartz, Alexander Hickey, Mangilal Agarwal, Hamid Dalir. Experimental and Computational Verification of Additively Manufactured Carbon Fiber and Nanoreinforced Filaments for Automotive Applications *Accepted*

Posters:

1. Oluwaseun Omole, Hamid Dalir. Analysis of Process Induced Deformations in Composite Manufacturing IUPUI Center for Research and Learning Symposium 2019, Indianapolis, IN, July 2019
2. Oluwaseun Omole, Hamid Dalir. Analysis of Process Induced Deformations in Composite Manufacturing, Louis Stokes Midwest Regional Center of Excellence, Indianapolis, IN, October 2019

Oral Presentations:

1. **Oluwaseun Omole**, Pias Kumar Biswas, Hamid Dalir, The Feasibility of Multiple Extruders in Additive Manufacturing, National Council for Undergraduate Research 2021 @Home, April 2021

2. **Oluwaseun Peter Omole**, Pias Kumar Biswas, Asel Habarakada Liyanage, Hamid Dalir. Further Optimization of Carbon Fiber Through Electrospinning Nanoparticles, AIAA Region III Conference, Purdue University, March 2022.

REFERENCES

1. Wable, V., et al., *Engineering the electrospinning of MWCNTs/epoxy nanofiber scaffolds to enhance physical and mechanical properties of CFRPs.* Composites Science and Technology, 2021. **213**.

2. Aliahmad, N., et al., *Electrospun Thermosetting Carbon Nanotube–Epoxy Nanofibers.* ACS Applied Polymer Materials, 2021. **3**(2): p. 610-619.

3. Aliahmad, N., et al., *Synthesis of V2O5/Single-Walled Carbon Nanotubes Integrated into Nanostructured Composites as Cathode Materials in High Performance Lithium-Ion Batteries.* 2022. **15**(2): p. 552.

4. Keyte, J., K. Pancholi, and J. Njuguna, *Recent Developments in Graphene Oxide/Epoxy Carbon Fiber-Reinforced Composites.* 2019. **6**.

5. Bacon, R., *Growth, Structure, and Properties of Graphite Whiskers.* Journal of Applied Physics, 1960. **31**(2): p. 283-290.

6. Bacon, R. and M.M. Tang, *Carbonization of cellulose fibers—II. Physical property study.* Carbon, 1964. **2**(3): p. 221-225.

7. Schalamon, W. and R. Bacon, *PROCESS FOR PRODUCING CARBON FIBERS HAVING A HIGH YOUNG'S MODULUS OF ELAST CITY* U.S. Patent, Editor. 1970, Union Carbide Corporation: United States. p. 4.

8. Tanaka, F. and T. Okabe, *1.4 Historical Review of Processing, Microstructures, and Mechanical Properties of PAN-Based Carbon Fibers,* in *Comprehensive Composite Materials II*, P.W.R. Beaumont and C.H. Zweben, Editors. 2018, Elsevier: Oxford. p. 66-85.

9. Johnson, D.J., *Structure and Properties of Carbon Fibres*, in *Carbon Fibers Filaments and Composites*, J.L. Figueiredo, et al., Editors. 1990, Springer Netherlands: Dordrecht. p. 119-146.

10. Peng, S., H. Shao, and X. Hu, *Lyocell fibers as the precursor of carbon fibers.* Journal of Applied Polymer Science, 2003. **90**(7): p. 1941-1947.

11. Inagaki, M., *CHAPTER 4 - Carbon Fibers*, in *New Carbons - Control of Structure and Functions*, M. Inagaki, Editor. 2000, Elsevier Science: Oxford. p. 82-123.

12. Mohee, F.M., A. Al-Mayah, and A. Plumtree, *Anchors for CFRP plates: State-of-the-art review and future potential.* Composites Part B: Engineering, 2016. **90**: p. 432-442.

13. Biswas, P.K., et al., *Higher strength carbon fiber lithium-ion polymer battery embedded multifunctional composites for structural applications.* Polymer Composites, 2022. **43**(5): p. 2952-2962.

14. Aliahmad, N., et al., *Carbon nanotube/epoxy submicron filaments for composite reinforcement applications*, in *AIAA Scitech 2021 Forum*. 2021, American Institute of Aeronautics and Astronautics.

15. Liyanage, A.A.H., et al., *Engineering uniformity in mass production of MWCNTs/epoxy nanofibers using a lateral belt-driven multi-nozzle electrospinning technique to enhance the mechanical properties of CFRPs.* Polymer Testing, 2023. **118**: p. 107883.

16. Biswas, P.K., et al., *Carbon and cellulose based nanofillers reinforcement to strengthen carbon fiber-epoxy composites: Processing, characterizations, and applications.* Frontiers in Materials, 2023. **9**.

17. Gogoi, R., A.K. Maurya, and G. Manik, *A review on recent development in carbon fiber reinforced polyolefin composites.* Composites Part C: Open Access, 2022. **8**: p. 100279.

18. Roberts, A., *The Carbon Fibre Industry Worldwide 2008-2014".* Innovation in Textiles, 2009. **4**.

19. Hollaway, L.C., *The evolution of and the way forward for advanced polymer composites in the civil infrastructure.* Construction and Building Materials, 2003. **17**(6): p. 365-378.

20. Van Den Einde, L., L. Zhao, and F. Seible, *Use of FRP composites in civil structural applications.* Construction and Building Materials, 2003. **17**(6): p. 389-403.

21. Sadeghian, P., A.R. Rahai, and M.R. Ehsani, *Effect of fiber orientation on compressive behavior of CFRP-confined concrete columns.* Journal of Reinforced Plastics and Composites, 2010. **29**(9): p. 1335-1346.

22. Mehdi, H. and R. Resatoglu, *Confinement of concrete columns using CFRP and expanded grout.* Journal of Structural Integrity and Maintenance, 2022. **7**(2): p. 128-135.

23. Ueda, T. and Y. Sato, *New Approach for Usage of Continuous Fiber as Non-Metallic Reinforcement of Concrete.* Structural Engineering International, 2002. **12**(2): p. 111-116.

24. Xu, X., et al., *Cellulose Nanocrystals vs. Cellulose Nanofibrils: A Comparative Study on Their Microstructures and Effects as Polymer Reinforcing Agents.* ACS Applied Materials & Interfaces, 2013. **5**(8): p. 2999-3009.

25. Alves, C., et al., *Ecodesign of automotive components making use of natural jute fiber composites.* 2010. **18**(4): p. 313-327.

26. Koronis, G., A. Silva, and M. Fontul, *Green composites: A review of adequate materials for automotive applications.* Composites Part B: Engineering, 2013. **44**(1): p. 120-127.

27. Zbiciak, A. and T. Markiewicz, *A new extraordinary means of appeal in the Polish criminal procedure: the basic principles of a fair trial and a complaint against a cassatory judgment.* Access to Justice in Eastern Europe, 2023. **6**(2): p. 1-18.

28. Ravishankar, B., S.K. Nayak, and M.A. Kader, *Hybrid composites for automotive applications – A review.* Journal of Reinforced Plastics and Composites, 2019. **38**(18): p. 835-845.

29. Koniuszewska, A.G. and J.W. Kaczmar, *Application of Polymer Based Composite Materials in Transportation.* Progress in Rubber, Plastics and Recycling Technology, 2016. **32**(1): p. 1-23.

30. Perner, M., et al., *Avoiding defects in manufacturing processes: A review for automated CFRP production.* Robotics and Computer-Integrated Manufacturing, 2016. **38**: p. 82-92.

31. Yang, H., G.J.I.f.s. Frye, and S. technology, *Polyamide fibers.* 1998. **15**.

32. Maria, M., *Advanced composite materials of the future in aerospace industry.* INCAS BULLETIN, 2013. **5**: p. 139-150.

33. Gerard, H.G., *Boeing and the 787 Dreamliner*, in *Decisions: An Engineering and Management Perspective*. 2015, IEEE. p. 187-218.

34. Marsh, G., *Airbus takes on Boeing with reinforced plastic A350 XWB.* Reinforced Plastics, 2007. **51**(11): p. 26-29.

35. Windhorst, T. and G. Blount, *Carbon-carbon composites: a summary of recent developments and applications.* Materials & Design, 1997. **18**(1): p. 11-15.

36. Lewis, S.J., *The use of carbon fibre composites on military aircraft.* Composites Manufacturing, 1994. **5**(2): p. 95-103.

37. Mason, R.B., et al., *Composites for military equipment.* Advanced Materials & Processes, 2004. **162**: p. 37+.

38. Shawbury, ed. *Polyamides as Engineering Thermoplastic Materials*. Rapra Review Reports. Vol. 11. 2000, Rapra Technology Limited. 129.

39. Francisco, D.L., L.B. Paiva, and W. Aldeia, *Advances in polyamide nanocomposites: A review.* Polymer Composites, 2019. **40**(3): p. 851-870.

40. García-López, D., et al., *Effect of organic modification of sepiolite for PA 6 polymer/organoclay nanocomposites.* Composites Science and Technology, 2010. **70**(10): p. 1429-1436.

41. Gupta, B., L. Marie-France, and P. Krawczak, *Polyamide-6/Clay Nanocomposites: A Critical Review.* Polymers & Polymer Composites, 2006. **14**(1): p. 13-38.

42. Dul, S., L. Fambri, and A. Pegoretti, *Fused deposition modelling with ABS–graphene nanocomposites.* Composites Part A: Applied Science and Manufacturing, 2016. **85**: p. 181-191.

43. Espera Jr, A.H., et al., *3D Printing of a Robust Polyamide-12-Carbon Black Composite via Selective Laser Sintering: Thermal and Electrical Conductivity.* Macromolecular Materials and Engineering, 2019. **304**(4): p. 1800718.

44. Chunze, Y., et al., *A Nanosilica/Nylon-12 Composite Powder for Selective Laser Sintering.* Journal of Reinforced Plastics and Composites, 2008. **28**(23): p. 2889-2902.

45. Masood, S.H. and W.Q. Song, *Development of new metal/polymer materials for rapid tooling using Fused deposition modelling.* Materials & Design, 2004. **25**(7): p. 587-594.

46. Hull, C.W., *Apparatus for production of three-dimensional objects by stereolithography*, USPTO, Editor. 1986, 3D Systems Inc: United States.

47. Watson, J.K. and K.M.B. Taminger, *A decision-support model for selecting additive manufacturing versus subtractive manufacturing based on energy consumption.* Journal of Cleaner Production, 2018. **176**: p. 1316-1322.

48. Gibson, I., et al., *Introduction and Basic Principles*, in *Additive Manufacturing Technologies*, I. Gibson, et al., Editors. 2021, Springer International Publishing: Cham. p. 1-21.

49. Jörg Bromberger, J.I., and Ana Maria Miranda, *The mainstreaming of additive manufacturing*. 2022, McKinsey & Company: McKinsey & Company.

50. Brenken, B., et al., *Fused filament fabrication of fiber-reinforced polymers: A review.* Additive Manufacturing, 2018. **21**: p. 1-16.

51. Gajdoš, I., et al., *Surface Finish Techniques for FDM Parts.* Materials Science Forum, 2015. **818**: p. 45-48.

52. Gunaydin, K. and H. Türkmen, *Common FDM 3D Printing Defects*. 2018.

53. Ahassen, A.A.e.a., *THE DURABILITY OF LARGE-SCALE ADDITIVE MANUFACTURING COMPOSITE MOLDS*, in *CAMX – The Composites and Advanced Materials Expo*. 2016, U.S. Government: Anaheim, CA.

54. Ning, F., et al., *Additive manufacturing of carbon fiber reinforced thermoplastic composites using fused deposition modeling.* Composites Part B: Engineering, 2015. **80**: p. 369-378.

55. Ferreira, R.T.L., et al., *Experimental characterization and micrography of 3D printed PLA and PLA reinforced with short carbon fibers.* Composites Part B: Engineering, 2017. **124**: p. 88-100.

56. Deka, A. and S. Behdad, *Part Separation Technique for Assembly-Based Design in Additive Manufacturing using Genetic Algorithm.* Procedia Manufacturing, 2019. **34**: p. 764-771.

57. Tian, X., et al., *Interface and performance of 3D printed continuous carbon fiber reinforced PLA composites.* Composites Part A: Applied Science and Manufacturing, 2016. **88**: p. 198-205.

58. Tian, X., et al., *Recycling and remanufacturing of 3D printed continuous carbon fiber reinforced PLA composites.* Journal of Cleaner Production, 2017. **142**: p. 1609-1618.

59. Matsuzaki, R., et al., *Three-dimensional printing of continuous-fiber composites by in-nozzle impregnation.* Scientific Reports, 2016. **6**(1): p. 23058.

60. Hou, Z., et al., *3D printed continuous fibre reinforced composite corrugated structure.* Composite Structures, 2018. **184**: p. 1005-1010.

61. Sugiyama, K., et al., *3D printing of composite sandwich structures using continuous carbon fiber and fiber tension.* Composites Part A: Applied Science and Manufacturing, 2018. **113**: p. 114-121.

62. Chen, G., et al., *High performance polyphenylene sulfide bio-composites with lightweight and sustainable hybrid fillers: biocarbon and recycled carbon fibers.* Composites Part C: Open Access, 2023: p. 100375.

63. Mosleh, N., A.M. Rezadoust, and S. Dariushi, *Determining process-window for manufacturing of continuous carbon fiber-reinforced composite Using 3D-printing.* Materials and Manufacturing Processes, 2021. **36**(4): p. 409-418.

64. Mori, K.-i., T. Maeno, and Y. Nakagawa, *Dieless Forming of Carbon Fibre Reinforced Plastic Parts Using 3D Printer.* Procedia Engineering, 2014. **81**: p. 1595-1600.

65. Nakagawa, Y., K.-i. Mori, and T. Maeno, *3D printing of carbon fibre-reinforced plastic parts.* The International Journal of Advanced Manufacturing Technology, 2017. **91**(5): p. 2811-2817.

66. Fujihara, K., et al., *Influence of processing conditions on bending property of continuous carbon fiber reinforced PEEK composites.* Composites Science and Technology, 2004. **64**(16): p. 2525-2534.

67. Dickson, A.N., K.-A. Ross, and D.P. Dowling, *Additive manufacturing of woven carbon fibre polymer composites.* Composite Structures, 2018. **206**: p. 637-643.

68. Dickson, A.N. and D.P. Dowling, *Enhancing the bearing strength of woven carbon fibre thermoplastic composites through additive manufacturing.* Composite Structures, 2019. **212**: p. 381-388.

69. Caminero, M.A., et al., *Impact damage resistance of 3D printed continuous fibre reinforced thermoplastic composites using fused deposition modelling.* Composites Part B: Engineering, 2018. **148**: p. 93-103.

70. Naranjo-Lozada, J., et al., *Tensile properties and failure behavior of chopped and continuous carbon fiber composites produced by additive manufacturing.* Additive Manufacturing, 2019. **26**: p. 227-241.

71. Pyl, L., K.-A. Kalteremidou, and D. Van Hemelrijck, *Exploration of the design freedom of 3D printed continuous fibre-reinforced polymers in open-hole tensile strength tests.* Composites Science and Technology, 2019. **171**: p. 135-151.

72. Chabaud, G., et al., *Hygromechanical properties of 3D printed continuous carbon and glass fibre reinforced polyamide composite for outdoor structural applications.* Additive Manufacturing, 2019. **26**: p. 94-105.

73. Goh, G.D., et al., *Characterization of mechanical properties and fracture mode of additively manufactured carbon fiber and glass fiber reinforced thermoplastics.* Materials & Design, 2018. **137**: p. 79-89.

74. Mohammadizadeh, M., et al., *3D printed fiber reinforced polymer composites - Structural analysis.* Composites Part B: Engineering, 2019. **175**: p. 107112.

75. Justo, J., et al., *Characterization of 3D printed long fibre reinforced composites.* Composite Structures, 2018. **185**: p. 537-548.

76. van de Werken, N., et al., *Design considerations and modeling of fiber reinforced 3D printed parts.* Composites Part B: Engineering, 2019. **160**: p. 684-692.

77. Ghebretinsae, F., O. Mikkelsen, and A.D. Akessa, *Strength analysis of 3D printed carbon fibre reinforced thermoplastic using experimental and numerical methods.* IOP Conference Series: Materials Science and Engineering, 2019. **700**(1): p. 012024.

78. Žmindák, M., et al., *Finite element simulation of tensile test of composite materials manufactured by 3D printing.* IOP Conference Series: Materials Science and Engineering, 2020. **776**(1): p. 012082.

79. Galvez, G.M., et al. *Finite Element Analysis of Different Infill Patterns for 3D Printed Tidal Turbine Blade*. Sustainability, 2023. **15**, DOI: 10.3390/su15010713.

80. Moldovan, C., et al., *FINITE ELEMENT ANALYSES OF 3D PRINTED COMPOSITE ROBOT COMPONENT.* ACTA TECHNICA NAPOCENSIS - Series: APPLIED MATHEMATICS, MECHANICS, and ENGINEERING; Vol 64, No 1 (2021): ACTA, 2021.

81. Avanzini, A., D. Battini, and L. Giorleo, *Finite element modelling of 3D printed continuous carbon fiber composites: Embedded elements technique and experimental validation.* Composite Structures, 2022. **292**: p. 115631.

82. Savandaiah, C., S. Sieberer, and G. Steinbichler *Additively Manufactured Composite Lug with Continuous Carbon Fibre Steering Based on Finite Element Analysis*. Materials, 2022. **15**, DOI: 10.3390/ma15051820.

83. Melenka, G.W., et al., *Evaluation and prediction of the tensile properties of continuous fiber-reinforced 3D printed structures.* Composite Structures, 2016. **153**: p. 866-875.

84. Al Abadi, H., et al., *Elastic properties of 3D printed fibre-reinforced structures.* Composite Structures, 2018. **193**: p. 8-18.